Since January 2020 Elsevier has created a COVID-19 resource centre with free information in English and Mandarin on the novel coronavirus COVID-19. The COVID-19 resource centre is hosted on Elsevier Connect, the company's public news and information website.

Informatics in Medicine Unlocked 28 (2022) 100849

Contents lists available at ScienceDirect

Informatics in Medicine Unlocked

journal homepage: www.elsevier.com/locate/imu

Optimal control analysis of a COVID-19 and tuberculosis co-dynamics model

M.S. Goudiaby [a,*], L.D. Gning [b], M.L. Diagne [c], Ben M. Dia [d], H. Rwezaura [e], J.M. Tchuenche [f]

[a] Département de Mathématiques, UFR des Sciences et Technologies, Université Assane Seck de Ziguinchor, BP 523, Ziguinchor, Senegal
[b] LERSTAD, UFR Sciences appliquées et Technologie, BP 234, Université Gaston Berger, Saint-Louis, Senegal
[c] Département de Mathématiques, UFR des Sciences et Technologies, Université de Thies, Thies, Senegal
[d] College of Petroleum Engineering and Geosciences (CPG), King Fahd University of Petroleum and Minerals (KFUPM), Dhahran 31261, Saudi Arabia
[e] Mathematics Department, University of Dar es Salaam, P.O. Box 35062, Dar es Salaam, Tanzania
[f] School of Computational and Communication Sciences and Engineering, Nelson Mandela African Institution of Science and Technology, P.O. Box 447, Arusha, Tanzania

ARTICLE INFO

Keywords:
Bifurcation
Co-infection
COVID-19
Optimal control
Reproduction number
Tuberculosis

ABSTRACT

Tuberculosis and COVID-19 are among the diseases with major global public health concern and great socio-economic impact. Co-infection of these two diseases is inevitable due to their geographical overlap, a potential double blow as their clinical similarities could hamper strategies to mitigate their spread and transmission dynamics. To theoretically investigate the impact of control measures on their long-term dynamics, we formulate and analyze a mathematical model for the co-infection of COVID-19 and tuberculosis. Basic properties of the tuberculosis only and COVID-19 only sub-models are investigated as well as bifurcation analysis (possibility of the co-existence of the disease-free and endemic equilibria). The disease-free and endemic equilibria are globally asymptotically stable. The model is extended into an optimal control system by incorporating five control measures. These are: tuberculosis awareness campaign, prevention against COVID-19 (e.g., face mask, physical distancing), control against co-infection, tuberculosis and COVID-19 treatment. Five strategies which are combinations of the control measures are investigated. Strategy B which focuses on COVID-19 prevention, treatment and control of co-infection yields a better outcome in terms of the number of COVID-19 cases prevented at a lower percentage of the total cost of this strategy.

1. Introduction

Mycobacterium tuberculosis is the causative agent of tuberculosis (TB), one of the top ten leading causes of death due to a single disease worldwide [1]. The transmission route are through cough, sneeze, speak or spit from active pulmonary TB persons, it can also be spread through use of an infected person's unsterilized eating utensils [2]. The chain of transmission could be broken by isolating and treating infectives [3].

On the other hand, COVID-19 caused by the coronavirus SARS-CoV-2 emerged in December 2019 [4–6], and spread worldwide like a wildfire [7]. The virus can spread from an infected person's mouth or nose when they cough, sneeze, speak, sing or breathe. These similarities of COVID-19 spreading pattern and TB call for great attention [8]. While most people who fall sick with COVID-19 may experience mild to moderate symptoms and recover without special treatment, the pandemic has claim millions of lives. COVID-19 prevention interventions (non-therapeutic measures) such as wearing face masks, self-isolation, physical distancing, and the most restrictive lock-downs could affect the transmission dynamic of TB. With the combination of non therapeutic prevention interventions and therapeutic measures, the number of COVID-19 cases and deaths have reduced despite the emergence of new variants of the COVID-19 virus [9].

Geographical overlap of both diseases and their clinical similarities could be a double blow in mitigating their spread because of the potential fatal outcome if they are not properly diagnosed and adequately treated [8]. Co-infection of both diseases is inevitable given the high worldwide prevalence of TB and COVID-19 [10–13]. Co-interaction of TB and COVID-19 may pose a challenge in mitigating their spread, as TB is a risk factor for COVID-19 both in terms of severity and mortality [14]. In fact, co-infection related mortality is higher (about 12.3%) in the patients with dual infection [15]. Also, COVID-19 patients have a low ability to build an immune response to TB, while in co-infected subjects, TB could impair the ability to mount a SARS-CoV-2 specific immune response [16]. These two diseases (TB and COVID-19) of global public health concern form a deadly duo, with great socio-economic impact worldwide [10]. From the aforementioned reasons, it is important to theoretically investigate the impact of control measures on their long-term dynamics.

* Corresponding author.
E-mail address: msgoudiaby@univ-zig.sn (M.S. Goudiaby).

https://doi.org/10.1016/j.imu.2022.100849
Received 9 December 2021; Received in revised form 2 January 2022; Accepted 2 January 2022
Available online 15 January 2022

We formulate and analyze a mathematical model for the co-infection of COVID-19 and TB transmission. Basic properties of the two sub-models, namely TB only and COVID-19 only) are investigated as well as the possibility of the co-existence of the disease-free and endemic equilibria (bifurcation analysis). Optimal control strategies are incorporated into the model, and conditions for the existence of optimal control and the optimality system for the co-infection model are established using the Pontryagin's maximum Principle.

The paper is organized as follows. The proposed co-infection model is formulated in Section 2. The model and its sub-models, TB and COVID-19 are rigorously analyzed in Section 3. In order to mitigate the spread of these two diseases and their co-infection, time variant controls are introduced into the full model, and the obtained optimal control problem investigated via the Pontryagin's Maximum Principle in Section 4. To support the theoretical results, numerical simulations are provided in Section NS, where five scenarios being combinations of various control strategies are investigated. Finally, Section 6 is the conclusion where it is noted that the best scenario in terms of the potential number of COVID-19 cases that could be prevented (at a lower percentage of the total cost) is Strategy B which focuses on COVID-19 prevention, treatment and control of co-infection.

2. The model

The population at time t denoted by $N(t)$ is divided into sub-populations of susceptible individuals $S(t)$, individuals exposed to COVID-19 only $E_c(t)$, unreported individuals infected with COVID-19 only $I_{CU}(t)$, reported individuals infected with COVID-19 only $I_{CR}(t)$, individuals exposed to tuberculosis only $E_T(t)$, unreported individuals infected with tuberculosis only $I_{TU}(t)$, reported individuals infected with tuberculosis only $I_{TR}(t)$, individuals exposed to tuberculosis and COVID-19 $E_{CT}(t)$, individuals infected with tuberculosis and COVID-19 $I_{CT}(t)$ and recovered individuals $R(t)$. It is important to note that all exposed individuals herein are actually asymptomatic and can transmit either of the disease as per their disease status.

The model has the following assumptions:

i. individuals infected with COVID-19 are susceptible to infection with tuberculosis and vice versa.
ii. co-infected individuals can transmit either COVID-19 or tuberculosis but not the mixed infections at the same time,
iii. co-infected individuals can recover either from COVID-19 or tuberculosis but not from the mixed infection at the same time,
iv. rate of transmissibility for singly infected and co-infected individuals are assumed to be the same.

Individuals are recruited into the population through birth or immigration at the rate ω_H. Susceptible humans S acquire COVID-19 following effective contacts with either singly or co-infected individuals with COVID-19 at the rate

$$\lambda_c = \frac{\Lambda_c(E_c + I_{CU})}{N}. \tag{1}$$

Similarly, the population S, is reduced due to infection with tuberculosis at the rate

$$\lambda_T = \frac{\Lambda_T I_{TU}}{N}. \tag{2}$$

From the model flow diagram in Fig. 1 and the above description, we derive the following nonlinear system ordinary differential equations for the COVID-19 and tuberculosis co-infection.

$$\begin{cases}
\frac{dS}{dt} = \omega_H + \omega_R R - \lambda_c S - \lambda_T S - \mu_H S,\\
\frac{dE_c}{dt} = \lambda_c S - \beta_c\lambda_c E_c - (\eta_R + \eta_U)E_c - \mu_H E_c,\\
\frac{dI_{CR}}{dt} = \eta_R E_c + \alpha_c I_{CT} - (\alpha_{CR} + \alpha_c)I_{CR} - (\mu_H + \phi_{CR})I_{CR},\\
\frac{dI_{CU}}{dt} = \eta_U E_c - (\gamma_{CU} + \alpha_{CU})I_{CU} - (\mu_H + \phi_{CU})I_{CU},\\
\frac{dE_{CT}}{dt} = \beta_c\lambda_c E_c + \beta_T\lambda_T E_T - \gamma_{CT}E_{CT} - \mu_H E_{CT},\\
\frac{dI_{CT}}{dt} = \gamma_{CT}E_{CT} + \gamma_{TU}I_{TU} + \gamma_{CU}I_{CU} + \alpha_{CR}I_{CR} + \alpha_{TR}I_{TR}\\
\qquad - (\alpha_c + \alpha_T)I_{CT} - (\mu_H + \phi_{CT})I_{CT},\\
\frac{dE_T}{dt} = \lambda_T S - (\beta_T\lambda_T + \theta_U + \theta_R)E_T - \mu_H E_T,\\
\frac{dI_{TU}}{dt} = \theta_U E_T - (\gamma_{TU} + \alpha_{TU})I_{TU} - (\mu_H + \phi_{TU})I_{TU},\\
\frac{dI_{TR}}{dt} = \theta_R E_T + \alpha_T I_{CT} - (\alpha_{TR} + \alpha_T)I_{TR} - (\mu_H + \phi_{TR})I_{TR},\\
\frac{dR}{dt} = \alpha_c I_{CR} + \alpha_{CU} I_{CU} + \alpha_{TU} I_{TU} + \alpha_T I_{TR} - \mu_H R - \omega_R R,
\end{cases} \tag{3}$$

together with initial conditions

$$\begin{aligned}
&S(0) \geq 0,\ E_c(0) \geq 0,\ E_T(0) \geq 0,\ E_{CT}(0) \geq 0,\ I_{CR}(0) \geq 0,\\
&I_{CU}(0) \geq 0, I_{CT}(0) \geq 0,\ I_{TU}(0) \geq 0,\ I_{TR}(0) \geq 0,\ R(0) \geq 0.
\end{aligned} \tag{4}$$

3. Model analysis

Two sub-models, namely: Tuberculosis only and COVID-19 only sub-models will first be considered.

3.1. COVID-19 only sub-model

By setting $E_T = E_{CT} = I_{CT} = I_{TU} = I_{TR} = 0$, we obtain the following COVID-19 only sub-model.

$$\begin{cases}
\frac{dS}{dt} = \omega_H + \omega_R R - \lambda_c S - \mu_H S,\\
\frac{dE_c}{dt} = \lambda_c S - (\eta_R + \eta_U + \mu_H)E_c,\\
\frac{dI_{CR}}{dt} = \eta_R E_c - (\alpha_c + \mu_H + \phi_{CR})I_{CR},\\
\frac{dI_{CU}}{dt} = \eta_U E_c - (\alpha_{CU} + \mu_H + \phi_{CU})I_{CU},\\
\frac{dR}{dt} = \alpha_c I_{CR} + \alpha_{CU} I_{CU} - \mu_H R - \omega_R R,
\end{cases} \tag{5}$$

where $N_c = S + E_c + I_{CR} + I_{CU} + R$. By adding up all the equations of the system (5), we have

$$\dot{N}_c = \omega_H - \mu_H N_c - \phi_{CR} I_{CR} - \phi_{CU} I_{CU} \leqslant \omega_H - \mu_H N_c. \tag{6}$$

The given initial conditions of the sub-model system (5) ensure that $N(0) \geq 0$. Thus, the total human population is positive and bounded for all finite time $t > 0$. From the theory of differential inequality [31], we have

$$N_c(t) \leqslant N_c(0)e^{-\mu_H t} + \frac{\omega_H}{\mu_H}(1 - e^{-\mu_H t}). \tag{7}$$

As $t \to +\infty$, we obtain $0 \leq N_c(t) \leq \frac{\omega_H}{\mu_H}$. The feasible region of the COVID-19 only sub-model (5) is given by

$$\Omega_c = \left\{(S, E_c, I_{CR}, I_{CU}, R) \in \mathbb{R}^5_+ : N_c(t) \leq \frac{\omega_H}{\mu_H}\right\}. \tag{8}$$

The set Ω_c is positively invariant and attracting [32], and all solutions of the COVID-19 only sub-model (5) starting in Ω_c remain in Ω_c for all $t \geq 0$. Thus, the model (5) is mathematically and epidemiologically well-posed, and it is sufficient to study its dynamics in Ω_c [3,33].

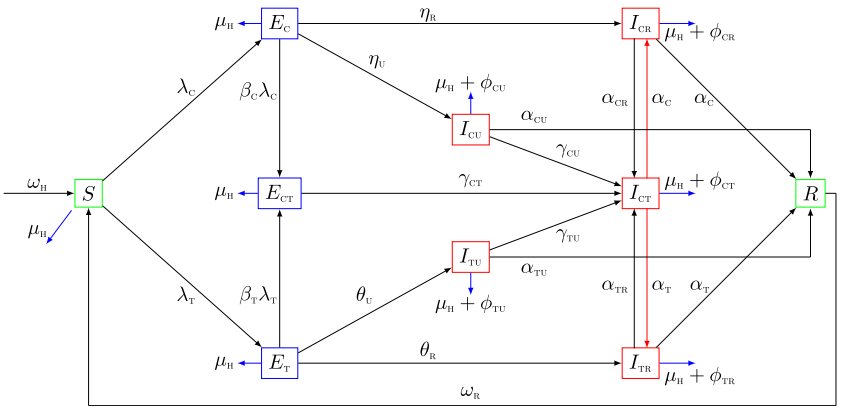

Fig. 1. COVID-19 and tuberculosis co-interaction flow diagram.

Table 1
Description of the variables and parameters.

Parameter	Interpretation	Value	Reference
ω_H	Recruitment rate	$\frac{10000}{59\times365}$	[17,18]
ω_R	Loss of immunity after recovery	0.1	Assumed
Λ_C	Effective contact rate transmission of COVID-19	0.6	[19]
Λ_T	Effective contact rate transmission of tuberculosis	1. 3	[20]
β_C	Modification parameter accounting for susceptibility of COVID-19-infected Individuals to tuberculosis	1	Assumed
β_T	Modification parameter accounting for susceptibility of tuberculosis-infected Individuals to COVID-19	1	Assumed
η_U	Progression rate from asymptomatic to unreported symptomatic COVID-19	0. 785	[21]
η_R	Progression rate from asymptomatic to reported symptomatic COVID-19	0. 2	[22]
θ_U	Progression rate from exposed to unreported infectious tuberculosis class	0.7	[23]
θ_R	Progression rate from exposed to reported infectious tuberculosis class	0.166	[23]
γ_{CT}	Fraction of individuals moving to the co-infection class	0.0333	Assumed
α_{CR}	Tuberculosis infection rate of reported individuals already infected with COVID-19	0.0028	Assumed
γ_{CU}	Tuberculosis infection rate of unreported individuals already infected with COVID-19	0.0044	Assumed
α_{TR}	COVID-19 infection rate of reported individuals already infected with tuberculosis	0.13	Assumed
γ_{TU}	COVID-19 infection rate of unreported individuals already infected with tuberculosis	0.0333	Assumed
α_{CU}	Recovery rate of unreported COVID-19 infected individuals	0.142	[21]
α_C	Recovery rate of reported COVID-19 infected individuals	0.68	[24]
α_{TU}	Recovery rate of unreported tuberculosis infected individuals	0.175	[25]
α_T	Recovery rate of reported tuberculosis infected individuals	0.35	[25]
ϕ_{CU}	Death rate of unreported COVID-19 infected individuals	0.0065	[26,27]
ϕ_{CR}	Death rate of reported COVID-19 infected individuals	0 .0018	[28]
ϕ_{TU}	Death rate of unreported tuberculosis infected individuals	0. 004	[29]
ϕ_{TR}	Death rate of reported tuberculosis infected individuals	0.000179	[30]
μ_H	Natural death rate of the population	$\frac{1}{59\times365}$	[17,18]

3.1.1. Stability of the disease-free equilibrium

The disease-free equilibrium (DFE) of the COVID-19 only sub-model system (5) is obtained when $E_c = I_{CR} = I_{CU} = R = 0$. Thus, the DFE of the COVID-19 only sub-model (5) is given by

$$\mathcal{E}_{C_0} = (S^0, E_c^0, I_{CR}^0, I_{CU}^0, R^0) = \left(\frac{\omega_H}{\mu_H}, 0, 0, 0, 0\right). \tag{9}$$

The linear stability of $\mathcal{E}_{C_0}$ is established using the next generation operator method on system (5) as described in [34]. System (5) can be written as

$$\dot{x} = f(x) = \mathcal{F}(x) - \mathcal{V}(x), \tag{10}$$

where

$$\mathcal{F} = \begin{pmatrix} \lambda_C S \\ 0 \\ 0 \end{pmatrix},$$

and

$$\mathcal{V} = \begin{pmatrix} (\eta_R + \eta_U + \mu_H)E_c \\ -\eta_R E_c + (\alpha_c + \mu_H + \phi_{CR})I_{CR} \\ -\eta_U E_c + (\alpha_{CU} + \mu_H + \phi_{CU})I_{CU} \end{pmatrix}.$$

are the new infection and transfer terms respectively. Evaluating the Jacobian of $\mathcal{F}$ and $\mathcal{V}$ at the DFE $\mathcal{E}_{C_0}$ gives

$$F = \begin{pmatrix} \Lambda_C & 0 & \Lambda_C \\ 0 & 0 & 0 \\ 0 & 0 & 0 \end{pmatrix},$$

and

$$V = \begin{pmatrix} \eta_R + \eta_U + \mu_H & 0 & 0 \\ -\eta_R & \alpha_c + \mu_H + \phi_{CR} & 0 \\ -\eta_U & 0 & \alpha_{CU} + \mu_H + \phi_{CU} \end{pmatrix}.$$

Set

$$A_1 = \eta_R + \eta_U + \mu_H,\ A_2 = \alpha_c + \mu_H + \phi_{CR} \text{ and } A_3 = \alpha_{CU} + \mu_H + \phi_{CU}. \tag{11}$$

The inverse of the matrix V is given by

$$V^{-1} = \begin{pmatrix} \frac{1}{A_1} & 0 & 0 \\ \frac{\eta_R}{A_1 A_2} & \frac{1}{A_2} & 0 \\ \frac{\eta_U}{A_1 A_3} & 0 & \frac{1}{A_3} \end{pmatrix}.$$

The largest eigenvalue of the next generation matrix FV^{-1} denoted by R_{0_C} is given by

$$R_{0_C} = \frac{\Lambda_c \eta_U}{A_1 A_3} + \frac{\Lambda_c}{A_1} = \frac{\Lambda_c(\eta_U + \alpha_{CU} + \mu_H + \phi_{CU})}{(\eta_R + \eta_U + \mu_H)(\alpha_{CU} + \mu_H + \phi_{CU})}. \tag{12}$$

The basic reproduction number R_{0_C} is defined as the expected number of secondary cases generated by one infected individual during its entire period of infectiousness in a fully susceptible population [34]. From Theorem 2 of [34], the following result follows.

Lemma 3.1. *The disease-free equilibrium $\mathcal{E}_{C_0}$ of the COVID-19 only sub-model system (5) is locally asymptotically stable if $R_{0_C} < 1$, and unstable otherwise.*

Proof. The stability of $\mathcal{E}_{C_0}$ is obtained from the roots of the characteristic polynomial, which states that the equilibrium is stable if the roots of the characteristic polynomial are all negative. For $\mathcal{E}_{C_0}$, the Jacobian matrix of the system is obtained as

$$J(\mathcal{E}_{C0}) = \begin{pmatrix} -\mu_H & -\Lambda_c & 0 & -\Lambda_c & \omega_R \\ 0 & \Lambda_c - A_1 & 0 & \Lambda_c & 0 \\ 0 & \eta_R & -A_2 & 0 & 0 \\ 0 & \eta_U & 0 & -A_3 & 0 \\ 0 & 0 & \alpha_c & \alpha_{CU} & -(\mu_H + \omega_R) \end{pmatrix}.$$

where $A_i; i = 1, 2, 3$ are given in (11). The characteristic polynomial is given by

$$\begin{aligned} P(\lambda) &= (\lambda + \mu_H)(\lambda + \mu_H + \omega_R)(-\lambda - A_2)((-\lambda + \Lambda_c - A_1)(-\lambda - A_3) - \Lambda_c \eta_U) \\ &= (\lambda + \mu_H)(\lambda + \mu_H + \omega_R)(-\lambda - A_2)(\lambda^2 + \lambda(A_1 - \Lambda_c + A_3) \\ &\quad + A_1 A_3 - \Lambda_c A_3 - \Lambda_c \eta_U). \end{aligned} \tag{13}$$

Using the Routh–Hurwitz criterion for second order polynomials, we have for $\Lambda_c < \eta_R + \eta_U + \mu_H$ and $R_{0_C} < 1$ that $A_1 - \Lambda_c + A_3$ and $A_1 A_3 - \Lambda_c A_3 - \Lambda_c \eta_U$ are positive. Hence all eigenvalues are negative which means that the DFE $\mathcal{E}_{C_0}$ of the COVID-19 only sub-model system (5) is locally asymptotically stable when $R_{0_C} < 1$. ■

Theorem 3.1. *The DFE of the COVID-19 only model (5) is globally asymptotically stable for if $R_{0_C} < 1$.*

Proof. Consider the following Lyapunov function

$$W = (\alpha_{CU} + \mu_H + \phi_{CU})E_c + \Lambda_c I_{CU}.$$

The time derivative of W computed along the solutions of (5) is given by

$$\begin{aligned} \dot{W} &= (\alpha_{CU} + \mu_H + \phi_{CU})\dot{E}_c + \Lambda_c \dot{I}_{CU}, \\ &= (\alpha_{CU} + \mu_H + \phi_{CU})\left[\lambda_c S - (\eta_R + \eta_U + \mu_H)E_c\right] + \\ &\quad \Lambda_c\left[\eta_U E_c - (\alpha_{CU} + \mu_H + \phi_{CU})I_{CU}\right], \\ &= (\alpha_{CU} + \mu_H + \phi_{CU})\left[\frac{\Lambda_c(E_c + I_{CU})}{N} S - (\eta_R + \eta_U + \mu_H)E_c\right] + \\ &\quad \Lambda_c\left[\eta_U E_c - (\alpha_{CU} + \mu_H + \phi_{CU})I_{CU}\right], \\ &\leqslant (\alpha_{CU} + \mu_H + \phi_{CU})\left[\Lambda_c(E_c + I_{CU}) - (\eta_R + \eta_U + \mu_H)E_c\right] + \\ &\quad \Lambda_c\left[\eta_U E_c - (\alpha_{CU} + \mu_H + \phi_{CU})I_{CU}\right], \\ &\leqslant (\alpha_{CU} + \mu_H + \phi_{CU})\Lambda_c E_c - (\eta_R + \eta_U + \mu_H)(\alpha_{CU} + \mu_H + \phi_{CU})E_c \\ &\quad + \Lambda_c \eta_U E_c, \\ &\leqslant \Lambda_c(\alpha_{CU} + \mu_H + \phi_{CU} + \eta_U)E_c - (\eta_R + \eta_U + \mu_H)(\alpha_{CU} + \mu_H + \phi_{CU})E_c, \\ &\leqslant (\eta_R + \eta_U + \mu_H)(\alpha_{CU} + \mu_H + \phi_{CU})E_c(R_{0_C} - 1), \\ &\leqslant 0, \quad \text{for } R_{0_C} \leqslant 1. \end{aligned}$$

Because all model parameters are non-negative, it follows that $\dot{W} \leqslant 0$ for $R_{0_C} \leqslant 1$, with $\dot{W} = 0$ if and only if $E_c = I_{CR} = I_{CU} = 0$. Substituting $(E_c, I_{CR}, I_{CU}) = (0, 0, 0)$ into 3.1 shows that $S \to \frac{\Pi_H}{\alpha_H}$ as $t \to \infty$. Hence, W is a Lyapunov function on Ω_c and the largest compact invariant set in $\{(S, E_c, I_{CR}, I_{CU}, R) \in \Omega_c : \dot{W} = 0\}$ is $\mathcal{E}_c$. Thus, by LaSalle's invariance principle, every solution of (5), with initial conditions in Ω_c approaches $\mathcal{E}_c$, as $t \to \infty$ whenever $R_{0_C} \leqslant 1$. ■

3.1.2. Stability of the endemic equilibrium

We explore the stability of the endemic equilibrium of the COVID-19 only sub-model system (5) given by

$$\begin{aligned} \mathcal{E}_{C_1} &= (S_{C_1}, E_{cC_1}, I_{CRC_1}, I_{CUC_1}, R_{C_1}), \\ &= \left(\frac{\omega_H}{\lambda_c^\star + \mu_H}, \frac{\omega_H \lambda_c^\star}{(\lambda_c^\star + \mu_H)A_1}, \frac{\omega_H \lambda_c^\star \eta_R}{(\lambda_c^\star + \mu_H)A_1 A_2}, \frac{\omega_H \lambda_c^\star \eta_U}{(\lambda_c^\star + \mu_H)A_1 A_3}, \right. \\ &\quad \left. \frac{\omega_H \lambda_c^\star(\alpha_c \eta_R A_3 + \alpha_{CU} \eta_U A_2)}{\mu_H(\lambda_c^\star + \mu_H)A_1 A_2 A_3}\right), \end{aligned} \tag{14}$$

where

$$\lambda_c^\star = \frac{\Lambda_c(E_{cC_1} + I_{CUC_1})}{S_{C_1} + E_{cC_1} + I_{CRC_1} + I_{CUC_1} + R_{C_1}}. \tag{15}$$

Note that

$$E_{cC_1} + I_{CUC_1} = \frac{\omega_H \lambda_c^\star A_2(A_3 + \eta_U)}{\mu_H(\lambda_c^\star + \mu_H)A_1 A_2 A_3}. \tag{16}$$

Also,

$$\begin{aligned} &S_{C_1} + E_{cC_1} + I_{CRC_1} + I_{CUC_1} + R_{C_1} \\ &= \frac{\lambda_c^\star\left(A_2 A_3 + \eta_R A_3\left(1 + \frac{\alpha_c}{\mu_H}\right) + \eta_U A_2\left(1 + \frac{\alpha_{CU}}{\mu_H}\right)\right) + A_1 A_2 A_3}{\mu_H(\lambda_c^\star + \mu_H)A_1 A_2 A_3}. \end{aligned} \tag{17}$$

Substituting Eqs. (16) and (18) into (15), we obtain

$$\lambda_c^\star\left(A_2 A_3 + \eta_R A_3\left(1 + \frac{\alpha_c}{\mu_H}\right) + \eta_U A_2\left(1 + \frac{\alpha_{CU}}{\mu_H}\right)\right) = \frac{A_2}{A_1 A_3}\left(R_{0_C} - 1\right). \tag{18}$$

Therefore, $\lambda_c^\star$ exists if and only if $R_{0_C} > 1$. Hence, the following result.

Theorem 3.2. *The COVID-19 only model system (5) has a unique endemic equilibrium if* $R_{0_C} > 1$.

In the following, we use the center manifold approach to analyze the global stability of the full model. To this end we use the notation: $x_1 = S$, $x_2 = E_c$, $x_3 = I_{CR}$, $x_4 = I_{CU}$, $x_5 = R$ and $N_c = x_1+x_2+x_3+x_4+x_5$ to write the model in the form $\dot{x} = f(x)$ with $x = (x_1, \dots, x_5)^T$ and $f = (f_1, \dots, f_5)$. That is

$$\begin{cases} \dot{x}_1 = f_1 &= \omega_H + \omega_R x_5 - \dfrac{\Lambda_c(x_2+x_4)}{x_1+x_2+x_3+x_4+x_5}x_1 - \mu_H x_1, \\ \dot{x}_2 = f_2 &= \dfrac{\Lambda_c(x_2+x_4)}{x_1+x_2+x_3+x_4+x_5}x_1 - (\eta_R+\eta_U+\mu_H)x_2, \\ \dot{x}_3 = f_3 &= \eta_R x_2 - (\alpha_c+\alpha_{CR}+\mu_H+\phi_{CR})x_3, \\ \dot{x}_4 = f_4 &= \eta_U x_2 - (\gamma_{CU}+\alpha_{CU}+\mu_H+\phi_{CU})x_4, \\ \dot{x}_5 = f_5 &= \alpha_c x_3 + \alpha_{CU}x_4 - (\mu_H+\omega_R)x_5, \end{cases} \tag{19}$$

The Jacobian of (19) at the DFE $\mathcal{E}_{C_0}$ is given by

$$J(\mathcal{E}_{C_0}) = \begin{pmatrix} -\mu_H & -\Lambda_c & 0 & -\Lambda_c & 0 \\ 0 & \Lambda_c - A_1 & 0 & \Lambda_c & 0 \\ 0 & \eta_R & -A_2 & 0 & 0 \\ 0 & \eta_U & 0 & -A_3 & 0 \\ 0 & 0 & \alpha_c & \alpha_{CU} & -\mu_H \end{pmatrix},$$

where $A_i; i = 1, 2, 3$ are given in Eq. (11).

We choose Λ_c as a bifurcation parameter. Therefore, setting $R_{0_C} = 1$, we obtain

$$\Lambda_c = \Lambda_c^\star = \frac{(\eta_R+\eta_U+\mu_H)(\alpha_{CU}+\mu_H+\phi_{CU})}{(\eta_U+\alpha_{CU}+\mu_H+\phi_{CU})}. \tag{20}$$

At $\Lambda_c = \Lambda_c^\star$, the Jacobian has a simple zero eigenvalue (since $A_1A_3 - \Lambda_c A_3 - \Lambda_c\eta_U = 0$, see Eq. (13)) and all other eigenvalues have negative real parts. Therefore, the DFE $\mathcal{E}_{C_0}$ is a non-hyperbolic equilibrium point. Hence, the center manifold theory [35] can be applied to model system (19) near $\Lambda_c = \Lambda_c^\star$.

The right eigenvector $w = (w_1, w_2, w_3, w_4, w_5)^T$ associated with the zero eigenvalue of $J(\mathcal{E}_{C_0})$ evaluated at $\Lambda_c = \Lambda_c^\star$ is

$$\begin{aligned} &w_1 = \left(\frac{\omega_R}{\mu_H+\omega_R}\left(\frac{\alpha_c\eta_R}{\mu_H A_2} + \frac{\alpha_{CU}\eta_U}{\mu_H A_3}\right) - \frac{A_1}{\mu_H}\right)w_2, \quad w_3 = \frac{\eta_R}{A_2}w_2, \\ &w_4 = \frac{\eta_U}{A_3}w_2, \quad w_5 = \frac{1}{\mu_H+\omega_R}\left(\frac{\alpha_c\eta_R}{A_2} + \frac{\alpha_{CU}\eta_U}{A_3}\right)w_2, \quad w_2 = w_2 > 0. \end{aligned} \tag{21}$$

Similarly, the left eigenvector $v = (v_1, v_2, v_3, v_4, v_5)$ is given by

$$v_1 = 0, \quad v_3 = 0, \quad v_5 = 0, \quad v_4 = \frac{A_1}{\eta_U+A_3}v_2, \quad v_2 = v_2 > 0. \tag{22}$$

The left and right eigenvectors satisfy $v.w = 1$ that is

$$v_2 w_2 \left(1 + \frac{\eta_U A_1}{(\eta_U+A_3)A_3}\right) = 1. \tag{23}$$

For the direction of the bifurcation, we determine the sign of the bifurcation parameters a and b. For a, one has

$$\begin{aligned} a &= \sum_{k,i,j=1}^{5} v_k w_i w_j \frac{\partial^2 f_k}{\partial x_i \partial x_j}(\mathcal{E}_{C_0}, \Lambda_c^\star), \\ &= \sum_{i,j=1}^{5} v_2 w_i w_j \frac{\partial^2 f_2}{\partial x_i \partial x_j}(\mathcal{E}_{C_0}, \Lambda_c^\star). \end{aligned} \tag{24}$$

The partial derivatives are

$$\begin{aligned} &\frac{\partial f_2}{\partial x_1} = \lambda_c - \lambda_c\frac{x_1}{N_c}, \quad \frac{\partial f_2}{\partial x_2} = (\Lambda_c - \lambda_c)\frac{x_1}{N_c}, \\ &\frac{\partial f_2}{\partial x_3} = -\lambda_c\frac{x_1}{N_c}, \quad \frac{\partial f_2}{\partial x_4} = (\Lambda_c - \lambda_c)\frac{x_1}{N_c}, \quad \frac{\partial f_2}{\partial x_5} = -\lambda_c\frac{x_1}{N_c}. \end{aligned} \tag{25}$$

Therefore,

$$\begin{aligned} a = \frac{\mu_H\Lambda_c^\star}{\omega_H}v_2(&w_1w_2 + w_1w_4 - w_2^2 - w_2w_3 - w_2w_4 \\ &- w_2w_5 - w_4w_2 - w_4w_3 - w_4^2 - w_4w_5). \end{aligned} \tag{26}$$

On the other hand, we have

$$\begin{aligned} w_1 &= \left(\frac{\omega_R}{\mu_H+\omega_R}\left(\frac{\alpha_c\eta_R}{\mu_H A_2} + \frac{\alpha_{CU}\eta_U}{\mu_H A_3}\right) - \frac{A_1}{\mu_H}\right)w_2, \\ &\leqslant \left(\frac{\alpha_c\eta_R}{\mu_H A_2} + \frac{\alpha_{CU}\eta_U}{\mu_H A_3} - \frac{A_1}{\mu_H}\right)w_2 \\ &\leqslant \frac{1}{\mu_H}\left[\left(\frac{\alpha_c}{A_2}-1\right)\eta_R + \left(\frac{\alpha_{CU}}{A_3}-1\right)\eta_U - \mu_H\right]w_2 \\ &\leqslant -\delta w_2. \end{aligned} \tag{27}$$

with

$$\delta = \frac{1}{\mu_H}\left[\left(1-\frac{\alpha_c}{A_2}\right)\eta_R + \left(1-\frac{\alpha_{CU}}{A_3}\right)\eta_U + \mu_H\right] > 0 \tag{28}$$

Taking into account (27) in (29), the bifurcation parameter a satisfies :

$$\begin{aligned} a \leqslant -\frac{\mu_H\Lambda_c^\star}{\omega_H}v_2(&\delta w_2^2 + \delta w_2w_4 + w_2^2 + w_2w_3 + w_2w_4 \\ &+ w_2w_5 + w_4w_2 + w_4w_3 + w_4^2 + w_4w_5), \\ \leqslant 0. \end{aligned} \tag{29}$$

For the bifurcation parameter b, we have

$$\begin{aligned} b &= \sum_{k,j=1}^{5} v_k w_j \frac{\partial^2 f_k}{\partial x_j \partial \Lambda_c}(\mathcal{E}_{C_0}, \Lambda_c^\star), \\ &= \sum_{j=1}^{5} v_2 w_j \frac{\partial^2 f_2}{\partial x_j \partial \Lambda_c}(\mathcal{E}_{C_0}, \Lambda_c^\star), \\ &= v_2w_2 + v_2w_4, \\ &= v_2w_2\left(1 + \frac{\eta_U}{A_3}\right) > 0. \end{aligned} \tag{30}$$

Since $a < 0$ and $b > 0$, the COVID-19 only sub-model system (5) does not exhibit the phenomenon of backward bifurcation at $R_{0_C} = 1$. Because the direction of the bifurcation is forward (transcritical bifurcation), a stable disease-free equilibrium cannot co-exist with a stable endemic equilibrium. Similar result for the COVID-19 only model was obtained in [36,37]. Hence, the following result.

Theorem 3.3. *The unique endemic equilibrium* $\mathcal{E}_{C_1}$ *of the COVID-19 only sub-model (5) is globally asymptotically stable if* $R_{0_C} > 1$.

The above result when $R_{0_C} > 1$ is graphically depicted in Fig. 2. The red line in Fig. 2 represents the area of instability of the endemic equilibrium $\mathcal{E}_{C_1}$, and the blue line the stability area of the endemic equilibrium $\mathcal{E}_{C_1}$. The red dotted line represents the threshold stability switch line $R_{0_C} = 1$. When $R_{0_C} > 1$, the green line does not cross the dotted line, hence the endemic equilibrium $\mathcal{E}_{C_1}$ is globally asymptotically stable.

3.2. Tuberculosis only sub-model

The following tuberculosis only sub-model is obtained from system (3) when $E_c = E_{CT} = I_{CT} = I_{CU} = I_{CR} = 0$.

$$\begin{cases} \dfrac{dS}{dt} = \omega_H - \lambda_T S - \mu_H S, \\ \dfrac{dE_T}{dt} = \lambda_T S - (\theta_U + \theta_R + \mu_H)E_T, \\ \dfrac{dI_{TU}}{dt} = \theta_U E_T - (\alpha_{TU} + \mu_H + \phi_{TU})I_{TU}, \\ \dfrac{dI_{TR}}{dt} = \theta_R E_T - (\alpha_T + \mu_H + \phi_{TR})I_{TR}, \\ \dfrac{dR}{dt} = \alpha_{TU}I_{TU} + \alpha_T I_{TR} - \mu_H R, \end{cases} \tag{31}$$

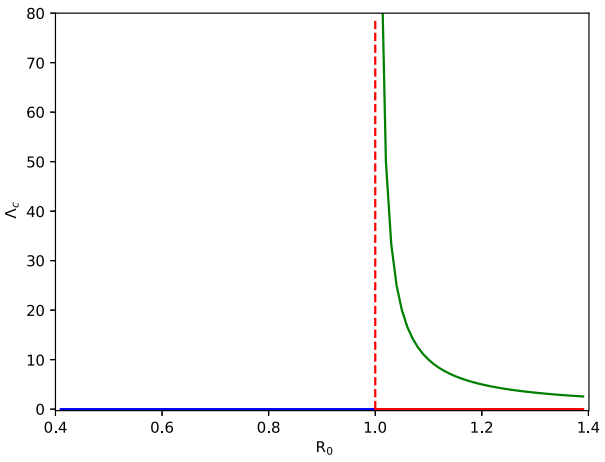

Fig. 2. Illustration of the bifurcation by plotting Λ_c versus R_{0_c}.

where $N_T = S + E_T + I_{TR} + I_{TU} + R$.

Arguing as in 3, the feasible region for the tuberculosis only sub-model

$$\Omega_T = \left\{ (S, E_T, I_{TU}, I_{TR}, R) \in \mathbb{R}^5_+ : N_T(t) \leq \frac{\omega_H}{\mu_H} \right\}. \tag{32}$$

is positively invariant and attracting, that is, solution starting in Ω_T will remain in Ω_T for all time $t \geq 0$. Thus, it is sufficient to consider the dynamics of the sub-model system (31) in Ω_T.

3.2.1. Stability of the disease-free equilibrium

The DFE of the tuberculosis only sub-model (31) is

$$\mathcal{E}_{T_0} = (S^0, E_T^0, I_{TU}^0, I_{TR}^0, R^0) = \left(\frac{\omega_H}{\mu_H}, 0, 0, 0, 0\right). \tag{33}$$

The basic reproductive number R_{0_T} is derived using the next generation operator method [34].

The sub-model system (31) can be written as

$$\dot{x} = f(x) = \mathcal{F}(x) - \mathcal{V}(x), \tag{34}$$

where

$$\mathcal{F} = \begin{pmatrix} \lambda_T S \\ 0 \\ 0 \end{pmatrix},$$

and

$$\mathcal{V} = \begin{pmatrix} (\theta_R + \theta_U + \mu_H)E_T \\ -\theta_U E_T + (\alpha_{TU} + \mu_H + \phi_{TU})I_{TU} \\ -\theta_R E_T + (\alpha_T + \mu_H + \phi_{TR})I_{TR} \end{pmatrix}$$

are the new infection and transfer terms respectively. Evaluating the Jacobian of $\mathcal{F}$ and $\mathcal{V}$ at the DFE $\mathcal{E}_{T_0}$ gives

$$F = \begin{pmatrix} 0 & \Lambda_T & 0 \\ 0 & 0 & 0 \\ 0 & 0 & 0 \end{pmatrix},$$

and

$$V = \begin{pmatrix} \theta_R + \theta_U + \mu_H & 0 & 0 \\ -\theta_U & \alpha_{TU} + \mu_H + \phi_{TU} & 0 \\ -\theta_R & 0 & \alpha_T + \mu_H + \phi_{TR} \end{pmatrix}.$$

Set

$$B_1 = \theta_R + \theta_U + \mu_H,\ B_2 = \alpha_{TU} + \mu_H + \phi_{TU} \text{ and } B_3 = \alpha_T + \mu_H + \phi_{TR}. \tag{35}$$

The inverse of the matrix V is

$$V^{-1} = \begin{pmatrix} \frac{1}{B_1} & 0 & 0 \\ \frac{\theta_U}{B_1 B_2} & \frac{1}{B_2} & 0 \\ \frac{\theta_R}{B_1 B_3} & 0 & \frac{1}{B_3} \end{pmatrix}.$$

Therefore, the basic reproduction number R_{0_T} which is the largest eigenvalue or spectral radius of the next generation matrix FV^{-1} is given by

$$R_{0_T} = \frac{\Lambda_T \theta_U}{B_1 B_2} = \frac{\Lambda_T \theta_U}{(\theta_R + \theta_U + \mu_H)(\alpha_{TU} + \mu_H + \phi_{TU})}. \tag{36}$$

The basic reproduction number R_{0_T} represents the average number of cases directly generated by one infectious TB case in a population which is assumed totally susceptible [38].

Thus, using Theorem 2 of [34], we establish the following result.

Theorem 3.4. *The DFE of the tuberculosis only sub-model (31) is locally asymptotically stable if $R_{0_T} < 1$, and unstable otherwise.*

Proof. For $\mathcal{E}_{T_0}$, the Jacobian matrix of the system is obtained as

$$J(\mathcal{E}_{T_0}) = \begin{pmatrix} -\mu_H & 0 & -\Lambda_T & 0 & \omega_R \\ 0 & -B_1 & \Lambda_T & 0 & 0 \\ 0 & \theta_U & -B_2 & 0 & 0 \\ 0 & \theta_R & 0 & -B_3 & 0 \\ 0 & 0 & \alpha_{TU} & \alpha_T & -\mu_H - \omega_R \end{pmatrix},$$

where $B_i;\ i = 1, 2, 3$ are given in Eq. (35). The characteristic polynomial is given by

$$\begin{aligned} P(\lambda) &= (\lambda + \mu_H)(\lambda + \mu_H + \omega_R)(-\lambda - B_3)((-\lambda - B_1)(-\lambda - B_2) - \Lambda_T \theta_U), \\ &= (\lambda + \mu_H)(\lambda + \mu_H + \omega_R)(-\lambda - B_3)(\lambda^2 + \lambda(B_1 + B_2) + B_1 B_2 - \Lambda_T \theta_U). \end{aligned} \tag{37}$$

The eigenvalues of the characteristic polynomial (37) are $-\mu_H$, $-\mu_H - \omega_R$, $-B_3$,

$$-(B_1+B_1)-\sqrt{(B_1 - B_1)^2 + 4\Lambda_T \theta_U} \quad \text{and} \quad -(B_1+B_1)+\sqrt{(B_1 - B_1)^2 + 4\Lambda_T \theta_U}.$$

The first four eigenvalues are negative, and since $R_{0_T} < 1$ the last one is also negative. Hence, the DFE $\mathcal{E}_{T_0}$ of the tuberculosis only sub-model system (31) is locally asymptotically stable when $R_{0_T} < 1$. ■

Theorem 3.5. *The DFE of the tuberculosis only sub-model (31) is globally asymptotically stable if $R_{0_T} < 1$, and unstable otherwise.*

Proof. Consider the following Lyapunov function

$$W = (\alpha_{TU} + \mu_H + \phi_{TU})E_T + \Lambda_T I_{TU}.$$

$$N_{T_1} = \frac{\omega_{H}\lambda_{T}^{\star}\left((\omega_{R}+\mu_{H})B_2B_3 + \theta_{R}B_2\left(\omega_{R}+\mu_{H}+\alpha_{T}\right) + \theta_{U}B_3\left(\omega_{R}+\mu_{H}+\alpha_{TU}\right)\right) + \omega_{H}(\omega_{R}+\mu_{H})B_1B_2B_3}{(\lambda_{T}^{\star}+\mu_{H})(\omega_{R}+\mu_{H})B_1B_2B_3 - \lambda_{T}^{\star}\omega_{R}(\alpha_{T}\theta_{R}B_2 + \alpha_{TU}\theta_{U}B_3)} \tag{40}$$

Box I.

The time derivative of W computed along the solutions of (31) is given by

$$\begin{aligned}
\dot{W} &= (\alpha_{TU}+\mu_{H}+\phi_{TU})\dot{E}_{T} + \Lambda_{T}\dot{I}_{TU},\\
&= (\alpha_{TU}+\mu_{H}+\phi_{TU})\left[\lambda_{T}S - (\theta_{R}+\theta_{U}+\mu_{H})E_{C}\right]\\
&\quad +\Lambda_{T}\left[\theta_{U}E_{T} - (\alpha_{TU}+\mu_{H}+\phi_{TU})I_{TU}\right],\\
&= (\alpha_{TU}+\mu_{H}+\phi_{TU})\left[\frac{\Lambda_{T}I_{CU}}{N}S - (\theta_{R}+\theta_{U}+\mu_{H})E_{T}\right]\\
&\quad +\Lambda_{T}\left[\theta_{U}E_{T} - (\alpha_{TU}+\mu_{H}+\phi_{TU})I_{TU}\right],\\
&\leqslant (\alpha_{TU}+\mu_{H}+\phi_{TU})\left[\Lambda_{T}I_{TU} - (\theta_{R}+\theta_{U}+\mu_{H})E_{T}\right]\\
&\quad +\Lambda_{T}\left[\theta_{U}E_{T} - (\alpha_{TU}+\mu_{H}+\phi_{TU})I_{TU}\right],\\
&\leqslant -(\alpha_{TU}+\mu_{H}+\phi_{TU})(\theta_{R}+\theta_{U}+\mu_{H})E_{T} + \Lambda_{T}\theta_{U}E_{T},\\
&\leqslant (\alpha_{TU}+\mu_{H}+\phi_{TU})(\theta_{R}+\theta_{U}+\mu_{H})E_{T}(R_{0_T}-1),\\
&\leqslant 0, \quad \text{for } R_{0_T}\leqslant 1.
\end{aligned}$$

Because all model parameters are non-negative, it follows that $\dot{W}$, for $R_{0_T}\leqslant 1$ with $\dot{W}=0$ if and only if $E_{T}=I_{TR}=I_{TU}=0$. Substituting $(E_{T}, I_{TR}, I_{TU}) = (0,0,0)$ into (31) shows that $S\to\frac{\omega_{H}}{\alpha_{H}}$ as $t\to\infty$. Hence, W is a Lyapunov function on Ω_T, and the largest compact invariant set in $\{(S,E_{T},I_{TR},I_{TU},R)\in\Omega_T : \dot{W}=0\}$ is $\mathcal{E}_T$. Thus, by LaSalle's invariance principle, every solution of (31), with initial conditions in Ω_T approaches $\mathcal{E}_T$, as $t\to\infty$ whenever $R_{0_T}\leqslant 1$. ■

3.2.2. Stability of the endemic equilibrium

We study the stability of the endemic equilibrium of the tuberculosis only sub-model system (31). From (5), this equilibrium denoted by $\mathcal{E}_{T_1}$ is given by

$$\begin{aligned}
S_{T_1} &= \frac{\omega_{H}(\omega_{R}+\mu_{H})B_1B_2B_3}{(\lambda_{T}^{\star}+\mu_{H})(\omega_{R}+\mu_{H})B_1B_2B_3 - \lambda_{T}^{\star}\omega_{R}(\alpha_{T}\theta_{R}B_2+\alpha_{TU}\theta_{U}B_3)},\\
E_{TT_1} &= \frac{\omega_{H}\lambda_{T}^{\star}(\omega_{R}+\mu_{H})B_2B_3}{(\lambda_{T}^{\star}+\mu_{H})(\omega_{R}+\mu_{H})B_1B_2B_3 - \lambda_{T}^{\star}\omega_{R}(\alpha_{T}\theta_{R}B_2+\alpha_{TU}\theta_{U}B_3)},\\
I_{TUT_1} &= \frac{\omega_{H}\lambda_{T}^{\star}\theta_{U}(\omega_{R}+\mu_{H})B_3}{(\lambda_{T}^{\star}+\mu_{H})(\omega_{R}+\mu_{H})B_1B_2B_3 - \lambda_{T}^{\star}\omega_{R}(\alpha_{T}\theta_{R}B_2+\alpha_{TU}\theta_{U}B_3)},\\
I_{TRT_1} &= \frac{\omega_{H}\lambda_{T}^{\star}\theta_{R}(\omega_{R}+\mu_{H})B_2}{(\lambda_{T}^{\star}+\mu_{H})(\omega_{R}+\mu_{H})B_1B_2B_3 - \lambda_{T}^{\star}\omega_{R}(\alpha_{T}\theta_{R}B_2+\alpha_{TU}\theta_{U}B_3)},\\
R_{T_1} &= \frac{\omega_{H}\lambda_{T}^{\star}(\alpha_{T}\theta_{R}B_2+\alpha_{TU}\theta_{U}B_3)}{(\lambda_{T}^{\star}+\mu_{H})(\omega_{R}+\mu_{H})B_1B_2B_3 - \lambda_{T}^{\star}\omega_{R}(\alpha_{T}\theta_{R}B_2+\alpha_{TU}\theta_{U}B_3)},
\end{aligned} \tag{38}$$

where

$$\begin{aligned}
\lambda_{T}^{\star} &= \frac{\Lambda_{T}I_{TUT_1}}{S_{T_1}+E_{TT_1}+I_{TUT_1}+I_{TRT_1}+R_{T_1}} = \frac{\Lambda_{T}I_{TUT_1}}{N_{T_1}},\\
&= \frac{\Lambda_{T}\omega_{H}\lambda_{T}^{\star}\theta_{U}(\omega_{R}+\mu_{H})B_3}{N_{T_1}(\lambda_{T}^{\star}+\mu_{H})(\omega_{R}+\mu_{H})B_1B_2B_3 - \lambda_{T}^{\star}\omega_{R}(\alpha_{T}\theta_{R}B_2+\alpha_{TU}\theta_{U}B_3)}
\end{aligned} \tag{39}$$

Note that N_{T_1} given in Box I.
Substituting (40) into (39), we obtain

$$\begin{aligned}
&\lambda_{T}^{\star}\left((\omega_{R}+\mu_{H})B_2B_3 + \theta_{R}B_2\left(\omega_{R}+\mu_{H}+\alpha_{T}\right) + \theta_{U}B_3\left(\omega_{R}+\mu_{H}+\alpha_{TU}\right)\right)\\
&= (\omega_{R}+\mu_{H})B_1B_2B_3\left(R_{0_T}-1\right).
\end{aligned} \tag{41}$$

Therefore, $\lambda_{T}^{\star}$ exist if and only if $R_{0_T}>1$. Hence, we have established the following result.

Theorem 3.6. *The tuberculosis only sub-model system (31) has one unique endemic equilibrium if* $R_{0_T}>1$.

We again use the center manifold approach to analyze the global stability of the tuberculosis only sub-model (31). To this end, we use the notation $x_1=S$, $x_2=E_{C}$, $x_3=I_{CT}$, $x_4=I_{CR}$, $x_5=R$ and $N_{T}=x_1+x_2+x_3+x_4+x_5$ to write the model in the form $\dot{x}=f(x)$, with $x=(x_1,\dots,x_5)^{T}$ and $f=(f_1,\dots,f_5)$ as follows

$$\begin{cases}
\dot{x}_1 = f_1 = \omega_{H} + \omega_{R}x_5 - \dfrac{\Lambda_{T}x_3}{x_1+x_2+x_3+x_4+x_5}x_1 - \mu_{H}x_1,\\
\dot{x}_2 = f_2 = \dfrac{\Lambda_{T}x_3}{x_1+x_2+x_3+x_4+x_5}x_1 - (\theta_{R}+\theta_{U}+\mu_{H})x_2,\\
\dot{x}_3 = f_3 = \theta_{U}x_2 - (\alpha_{TU}+\mu_{H}+\phi_{TU})x_3,\\
\dot{x}_4 = f_4 = \theta_{R}x_2 - (\alpha_{T}+\mu_{H}+\phi_{TR})x_4,\\
\dot{x}_5 = f_5 = \alpha_{TU}x_3 + \alpha_{T}x_4 - (\mu_{H}+\omega_{R})x_5,
\end{cases} \tag{42}$$

The Jacobian of (42) at the DFE $\mathcal{E}_{T_0}$ is

$$J(\mathcal{E}_{T_0}) = \begin{pmatrix}
-\mu_{H} & 0 & -\Lambda_{T} & 0 & \omega_{R}\\
0 & -B_1 & \Lambda_{T} & 0 & 0\\
0 & \theta_{U} & -B_2 & 0 & 0\\
0 & \theta_{R} & 0 & -B_3 & 0\\
0 & 0 & \alpha_{TU} & \alpha_{T} & -\mu_{H}-\omega_{R}
\end{pmatrix},$$

where $B_i;\ i=1,2,3$ are given in Eq. (35). We choose Λ_{T} as a bifurcation parameter. Therefore, setting $R_{0_T}=1$, we obtain

$$\Lambda_{T} = \Lambda_{T}^{\star} = \frac{B_1B_2}{\theta_{U}} = \frac{(\theta_{R}+\theta_{U}+\mu_{H})(\alpha_{TU}+\mu_{H}+\phi_{TU})}{\theta_{U}}. \tag{43}$$

At $\Lambda_{T}=\Lambda_{T}^{\star}$ the Jacobian has a simple zero eigenvalue and all other eigenvalues have negative real parts. Therefore, the disease free equilibrium point $\mathcal{E}_{T_0}$ is a non-hyperbolic equilibrium point. Hence, the center manifold theory can be applied to model system (42) near $\Lambda_{T}=\Lambda_{T}^{\star}$.

The right eigenvector $w=(w_1,w_2,w_3,w_4,w_5)^{T}$ associated with the zero eigenvalue of $J(\mathcal{E}_{T_0})$ evaluated at $\Lambda_{T}=\Lambda_{T}^{\star}$ is

$$\begin{aligned}
&w_1 = \frac{\omega_{R}}{\mu_{H}+\omega_{R}}\left(\frac{\alpha_{T}\theta_{R}}{\mu_{H}B_3} + \frac{\alpha_{TU}\eta_{U}}{\mu_{H}B_2}\right)w_2 - \frac{B_1}{\mu_{H}}w_2, \quad w_3 = \frac{\theta_{U}}{B_2}w_2, \quad w_4 = \frac{\theta_{R}}{B_3}w_2,\\
&w_5 = \frac{1}{\mu_{H}+\omega_{R}}\left(\frac{\alpha_{T}\theta_{R}}{B_3} + \frac{\alpha_{TU}\eta_{U}}{B_2}\right)w_2, \quad w_2 = w_2 > 0.
\end{aligned} \tag{44}$$

Similarly, the left eigenvector $v=(v_1,v_2,v_3,v_4,v_5)$ is given by

$$v_1=0, \quad v_4=0, \quad v_5=0, \quad v_3=\frac{B_1}{\theta_{U}}v_2, \quad v_2=v_2>0. \tag{45}$$

The left and right eigenvectors satisfy $v.w=1$, that is,

$$v_2w_2\left(1+\frac{B_1}{B_2}\right)=1. \tag{46}$$

For the direction of the bifurcation, we determine the sign of the bifurcation parameters a et b.

$$\begin{aligned} a &= \sum_{k,i,j=1}^{5} v_k w_i w_j \frac{\partial^2 f_k}{\partial x_i \partial x_j}(\mathcal{E}_{T_0}, \Lambda_T^\star) \\ &= \sum_{i,j=1}^{5} v_2 w_i w_j \frac{\partial^2 f_2}{\partial x_i \partial x_j}(\mathcal{E}_{T_0}, \Lambda_T^\star). \end{aligned} \tag{47}$$

The partial derivatives are

$$\begin{aligned} &\frac{\partial f_2}{\partial x_1} = \lambda_T - \lambda_T \frac{x_1}{N_T}, \quad \frac{\partial f_2}{\partial x_2} = -\lambda_T \frac{x_1}{N_T}, \\ &\frac{\partial f_2}{\partial x_3} = (\Lambda_T - \lambda_T)\frac{x_1}{N_T}, \quad \frac{\partial f_2}{\partial x_4} = -\lambda_T \frac{x_1}{N_T}, \quad \frac{\partial f_2}{\partial x_5} = -\lambda_T \frac{x_1}{N_T}. \end{aligned} \tag{48}$$

Therefore,

$$\begin{aligned} a &= \frac{\mu_H \Lambda_T^\star}{\omega_H} v_2 (w_1 w_3 + w_3 w_2 - w_3^2 - w_3 w_4 - w_3 w_5), \\ &= \frac{\mu_H \Lambda_T^\star}{\omega_H} \frac{\theta_U}{B_2} v_2 w_2^2 \left(-\frac{B_1}{\mu_H} - \frac{\theta_U}{B_2} - \frac{\theta_R}{B_3} - \frac{\alpha_T \theta_R}{\mu_H B_3} - \frac{\alpha_{TU} \eta_U}{\mu_H B_2} - 1 \right), \\ &= -\frac{\mu_H B_1}{\omega_H} v_2 w_2^2 \left(\frac{B_1}{\mu_H} + \frac{\theta_U}{B_2} + \frac{\theta_R}{B_3} + \frac{\alpha_T \theta_R}{\mu_H B_3} + \frac{\alpha_{TU} \eta_U}{\mu_H B_2} + 1 \right) < 0. \end{aligned} \tag{49}$$

For the bifurcation parameter b, we have

$$\begin{aligned} b &= \sum_{k,j=1}^{5} v_k w_j \frac{\partial^2 f_k}{\partial x_j \partial \Lambda_T}(\mathcal{E}_{T_0}, \Lambda_T^\star), \\ &= \sum_{j=1}^{5} v_2 w_j \frac{\partial^2 f_2}{\partial x_j \partial \Lambda_T}(\mathcal{E}_{T_0}, \Lambda_T^\star), \\ &= v_2 w_3, \\ &= \frac{\theta_U}{B_2} v_2 w_2 > 0. \end{aligned} \tag{50}$$

Since $a < 0$ and $b > 0$, our proposed tuberculosis only sub-model system (31) does not exhibit the phenomenon of backward bifurcation at $R_{0_T} = 1$. Hence, the following result.

Theorem 3.7. *The unique endemic equilibrium $\mathcal{E}_{T_1}$ of the tuberculosis only sub-model (31) is globally asymptotically stable if $R_{0_T} > 1$.*

The above result when $R_{0_T} > 1$ is graphically depicted in Fig. 3. The red line in Fig. 2 represents the stability area of the DFE $\mathcal{E}_{T_0}$, and the blue line is the instability area of the DFE. The red dotted line represents the threshold stability switch line $R_{0_T} = 1$. When $R_{0_T} > 1$, the green line does not cross the dotted line, hence the endemic equilibrium $\mathcal{E}_{T_1}$ is globally asymptotically stable.

3.3. Tuberculosis-COVID-19 model

The feasible region of the full model system (3) is

$$\Omega_{CT} = \Omega_C \times \Omega_T, \tag{51}$$

where Ω_C and Ω_T are defined in (8) and (32), respectively.

The DFE of the COVID-19 and tuberculosis co-infection model is given by

$$\mathcal{E}_0 = (S^0, E_C^0, I_{CR}^0, I_{CU}^0, E_{CT}^0, I_{CT}^0, E_T^0, I_{TU}^0, I_{TR}^0, R^0) = \left(\frac{\omega_H}{\mu_H}, 0, 0, 0, 0, 0, 0, 0, 0, 0 \right). \tag{52}$$

From the basic reproduction number of the COVID-19 only and tuberculosis only sub-models, the basic reproduction number of the full system is given as

$$R_{0_{CT}} = \max(R_{0_C}, R_{0_T}), \tag{53}$$

where R_{0_C} and R_{0_T} are respectively defined in (12) and (36).

Using Theorem 2 of [34],

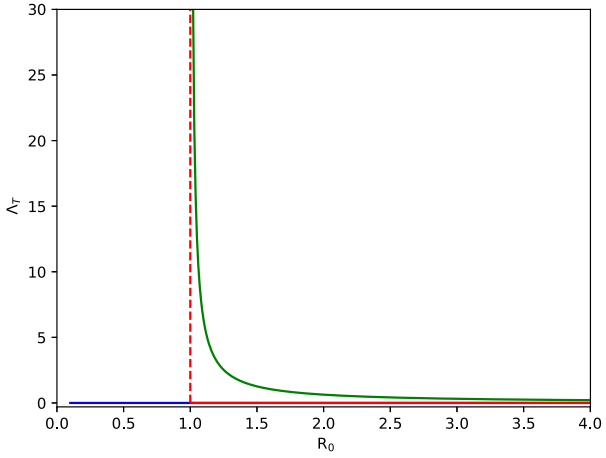

Fig. 3. Illustration of the bifurcation by plotting Λ_T versus R_{0_T}.

Theorem 3.8. *The DFE of the tuberculosis–COVID-19 model (31) is locally asymptotically stable if $R_{0_{CT}} < 1$, and unstable otherwise.*

Since the COVID-19 only and tuberculosis only sub-models do not undergo the phenomenon of backward bifurcation, the full tuberculosis–COVID-19 model will not undergo backward bifurcation.

4. Optimal control model

This section is devoted to investigating optimal interventions for mitigating the spread of COVID-19 and tuberculosis and their co-infection. We incorporate the following five controls into the full model (3)

u_1: Public awareness campaign control of tuberculosis,
u_2: Prevention control against COVID-19 (e.g., face mask, physical distancing),
u_3: Control against co-infection with a second disease,
u_4: Tuberculosis treatment control, and
u_5: COVID-19 treatment control.

The model system (3) now reads

$$\begin{cases} \frac{dS}{dt} = \omega_H + \omega_{CU} I_{CU} + \omega_{CR} I_{CR} + \omega_{TU} I_{TU} + \omega_{TR} I_{TR} \\ \qquad + \omega_{CT} I_{CT} - (1-u_2)\lambda_C S - (1-u_1)\lambda_T S - \mu_H S, \\ \frac{dE_C}{dt} = (1-u_2)\lambda_C S - (1-u_3)\beta_C \lambda_C E_C - (\eta_R + \eta_U) E_C - \mu_H E_C, \\ \frac{dI_{CR}}{dt} = \eta_R E_C + (1+u_5)\alpha_C I_{CT} - (\omega_{CR} + \alpha_{CR} + (1+u_5)\alpha_C) I_{CR} - (\mu_H + \phi_{CR}) I_{CR}, \\ \frac{dI_{CU}}{dt} = \eta_U E_C - (\omega_{CU} + \gamma_{CU} + \alpha_{CU}) I_{CU} - (\mu_H + \phi_{CU}) I_{CU}, \\ \frac{dE_{CT}}{dt} = (1-u_3)\beta_C \lambda_C E_C + (1-u_3)\beta_T \lambda_T E_T - \gamma_{CT} E_{CT} - \mu_H E_{CT}, \\ \frac{dI_{CT}}{dt} = \gamma_{CT} E_{CT} + \gamma_{TU} I_{TU} + \gamma_{CU} I_{CU} + \alpha_{CR} I_{CR} + \alpha_{TR} I_{TR} \\ \qquad - (\omega_{CT} + (1+u_5)\alpha_C + (1+u_4)\alpha_T) I_{CT} - (\mu_H + \phi_{CT}) I_{CT}, \\ \frac{dE_T}{dt} = (1-u_1)\lambda_T S - (1-u_3)\beta_T \lambda_T E_T - (\theta_U + \theta_R) E_T - \mu_H E_T, \\ \frac{dI_{TU}}{dt} = \theta_U E_T - (\omega_{TU} + \gamma_{TU} + \alpha_{TU}) I_{TU} - (\mu_H + \phi_{TU}) I_{TU}, \\ \frac{dI_{TR}}{dt} = \theta_R E_T + (1+u_4)\alpha_T I_{CT} - (\omega_{TR} + \alpha_{TR} + (1+u_4)\alpha_T) I_{TR} - (\mu_H + \phi_{TR}) I_{TR}, \\ \frac{dR}{dt} = (1+u_5)\alpha_C I_{CR} + \alpha_{CU} I_{CU} + \alpha_{TU} I_{TU} + (1+u_4)\alpha_T I_{TR} - \mu_H R, \end{cases} \tag{54}$$

with initial conditions

$$S(0)\geq 0,\ E_{c}(0)\geq 0,\ E_{T}(0)\geq 0,\ E_{CT}(0)\geq 0,\ I_{CR}(0)\geq 0,\\ I_{CU}(0)\geq 0, I_{CT}(0)\geq 0,\ I_{TU}(0)\geq 0,\ I_{TR}(0)\geq 0,\ R(0)\geq 0. \tag{55}$$

In what follows, because the positive balancing cost factors transfer the integral into monetary quantity over a finite period of time, we choose a quadratic control function, see [36] and the references therein. Thus, consider the following quadratic objective functional which measures the cost of the control. This cost includes strategies and treatment for mitigating at the population level the spread of COVID-19 and tuberculosis, as well as their co-infection. Thus, the nonlinear objective function is

$$J(u_1,u_2,u_3,u_4,u_5)=\int_0^T\Big[c_1E_c(t)+c_2E_{CT}(t)+c_3E_T(t)+c_4I_{CU}(t)+c_5I_{TU}(t)\\ +c_6I_{CR}(t)+c_7I_{CT}(t)+c_8I_{TR}(t)+\frac{w_1}{2}u_1^2\\ +\frac{w_2}{2}u_2^2+\frac{w_3}{2}u_3^2+\frac{w_4}{2}u_4^2+\frac{w_5}{2}u_5^2\Big]\,dt, \tag{56}$$

where T is the final time, $c_i,\ i=1,\dots,8$ are positive weight constants, and $w_i,\ i=1,\dots,5$ are weight constants for the strategies and treatments against proliferation of the COVID-19 and tuberculosis. The linear and quadratic form of the controls in (54) and in the objective function allow for the Hamiltonian associated to the optimal control problem to be maximized. Therefore, we seek to find, using the maximum principle of Pontryagin [39], an optimal control $(u_1^*,u_2^*,u_3^*,u_4^*,u_5^*)\in U$ satisfying (54), such that

$$J(u_1^*,u_2^*,u_3^*,u_4^*,u_5^*)=\min\{J(u_1,u_2,u_3,u_4,u_5)\mid(u_1,u_2,u_3,u_4,u_5)\in U\}. \tag{57}$$

The associated pseudo-Hamiltonian is

$$\begin{aligned}\mathbb{H}&=c_1E_c(t)+c_2E_{CT}(t)+c_3E_T(t)+c_4I_{CU}(t)\\ &\quad+c_5I_{TU}(t)+c_6I_{CR}(t)+c_7I_{CT}(t)+c_8I_{TR}(t)\\ &+\frac{w_1}{2}u_1^2+\frac{w_2}{2}u_2^2+\frac{w_3}{2}u_3^2+\frac{w_4}{2}u_4^2+\frac{w_5}{2}u_5^2\\ &+\xi_1\big(\omega_H+\omega_{CU}I_{CU}+\omega_{CR}I_{CR}+\omega_{TU}I_{TU}+\omega_{TR}I_{TR}+\omega_{CT}I_{CT}\\ &\quad-(1-u_2)\lambda_cS-(1-u_1)\lambda_TS-\mu_HS\big)\\ &+\xi_2\big((1-u_2)\lambda_cS-(1-u_3)\beta_c\lambda_cE_c-(\eta_R+\eta_U)E_c-\mu_HE_c\big)\\ &+\xi_3\big(\eta_RE_c+(1+u_5)\alpha_cI_{CT}-(\omega_{CR}+\alpha_{CR}+(1+u_5)\alpha_c)I_{CR}-(\mu_H+\phi_{CR})I_{CR}\big)\\ &+\xi_4\big(\eta_UE_c-(\omega_{CU}+\gamma_{CU}+\alpha_{CU})I_{CU}-(\mu_H+\phi_{CU})I_{CU}\big)\\ &+\xi_5\big((1-u_3)\beta_c\lambda_cE_c+(1-u_3)\beta_T\lambda_TE_T-\gamma_{CT}E_{CT}-\mu_HE_{CT}\big)\\ &+\xi_6\big(\gamma_{CT}E_{CT}+\gamma_{TU}I_{TU}+\gamma_{CU}I_{CU}+\alpha_{CR}I_{CR}+\alpha_{TR}I_{TR}\\ &\quad-(\omega_{CT}+(1+u_5)\alpha_c+(1+u_4)\alpha_T)I_{CT}-(\mu_H+\phi_{CT})I_{CT}\big)\\ &+\xi_7\big((1-u_1)\lambda_TS-(1-u_3)\beta_T\lambda_TE_T-(\theta_U+\theta_R)E_T-\mu_HE_T\big)\\ &+\xi_8\big(\theta_UE_T-(\omega_{TU}+\gamma_{TU}+\alpha_{TU})I_{TU}-(\mu_H+\phi_{TU})I_{TU}\big)\\ &+\xi_9\big(\theta_RE_T+(1+u_4)\alpha_TI_{CT}-(\omega_{TR}+\alpha_{TR}+(1+u_4)\alpha_T)I_{TR}-(\mu_H+\phi_{TR})I_{TR}\big)\\ &+\xi_{10}\big((1+u_5)\alpha_cI_{CR}+\alpha_{CU}I_{CU}+\alpha_{TU}I_{TU}+(1+u_4)\alpha_TI_{TR}-\mu_HR\big),\end{aligned} \tag{58}$$

where $\xi_i,\ i=1,\dots,10$ are the adjoint variables satisfying

$$\begin{aligned}\xi_1'&=-\frac{\partial\mathbb{H}}{\partial S} & \xi_2'&=-\frac{\partial\mathbb{H}}{\partial E_c},\\ \xi_3'&=-\frac{\partial\mathbb{H}}{\partial I_{CR}} & \xi_4'&=-\frac{\partial\mathbb{H}}{\partial I_{CU}},\\ \xi_5'&=-\frac{\partial\mathbb{H}}{\partial E_{CT}} & \xi_6'&=-\frac{\partial\mathbb{H}}{\partial I_{CT}},\\ \xi_7'&=-\frac{\partial\mathbb{H}}{\partial E_T} & \xi_8'&=-\frac{\partial\mathbb{H}}{\partial I_{TU}},\\ \xi_9'&=-\frac{\partial\mathbb{H}}{\partial I_{TR}} & \xi_{10}'&=-\frac{\partial\mathbb{H}}{\partial R}.\end{aligned} \tag{59}$$

Writing (61) in details gives

$$\begin{cases}\dot\xi_1=(1-u_2)\lambda_c(\xi_1-\xi_2)\left(1-\frac{S}{N}\right)+(1-u_1)\lambda_T(\xi_1-\xi_7)\left(1-\frac{S}{N}\right)\\ \quad+(1-u_3)\beta_c\lambda_c(\xi_5-\xi_2)\frac{E_c}{N}\\ \quad+(1-u_3)\beta_T\lambda_T(\xi_5-\xi_7)\frac{E_T}{N}+\mu_H\xi_1,\\ \dot\xi_2=(1-u_2)(\Lambda_c-\lambda_c)(\xi_1-\xi_2)\frac{S}{N}+(1-u_1)\lambda_T(\xi_7-\xi_1)\frac{S}{N}\\ \quad+(1-u_3)\beta_c(\Lambda_c-\lambda_c)(\xi_2-\xi_5)\frac{E_c}{N}\\ \quad+(1-u_3)\beta_c\lambda_c(\xi_2-\xi_5)+(1-u_3)\beta_T\lambda_T(\xi_5-\xi_7)\frac{E_T}{N}\\ \quad+(\xi_2-\xi_3)\eta_R+(\xi_2-\xi_4)\eta_U+\mu_H\xi_2-c_1,\\ \dot\xi_3=(1-u_2)\lambda_c(\xi_2-\xi_1)\frac{S}{N}+(1-u_1)\lambda_T(\xi_7-\xi_1)\frac{S}{N}\\ \quad+(1-u_3)\beta_c\lambda_c(\xi_5-\xi_2)\frac{E_c}{N}+(\mu_H+\phi_{CR})\xi_3\\ \quad+(1-u_3)\beta_T\lambda_T(\xi_5-\xi_7)\frac{E_T}{N}+\alpha_{CR}(\xi_3-\xi_6)\\ \quad+\omega_{CR}(\xi_3-\xi_1)+(1+u_5)\alpha_c(\xi_3-\xi_{10})-c_6,\\ \dot\xi_4=(1-u_2)(\Lambda_c-\lambda_c)(\xi_1-\xi_2)\frac{S}{N}+(1-u_1)\lambda_T(\xi_7-\xi_1)\frac{S}{N}\\ \quad+(1-u_3)\beta_c(\Lambda_c-\lambda_c)(\xi_2-\xi_5)\frac{E_c}{N}\\ \quad+(1-u_3)\beta_T\lambda_T(\xi_5-\xi_7)\frac{E_T}{N}+\alpha_{CU}(\xi_4-\xi_{10})+\omega_{CU}(\xi_4-\xi_1)\\ \quad+\gamma_{CU}(\xi_4-\xi_6)+(\mu_H+\phi_{CU})\xi_4-c_4,\\ \dot\xi_5=(1-u_2)\lambda_c(\xi_2-\xi_1)\frac{S}{N}+(1-u_1)\lambda_T(\xi_7-\xi_1)\frac{S}{N}\\ \quad+(1-u_3)\beta_c\lambda_c(\xi_5-\xi_2)\frac{E_c}{N}\\ \quad+(1-u_3)\beta_T\lambda_T(\xi_5-\xi_7)\frac{E_T}{N}+\gamma_{CT}(\xi_5-\xi_6)+\mu_H\xi_5-c_2,\\ \dot\xi_6=(1-u_2)\lambda_c(\xi_2-\xi_1)\frac{S}{N}+(1-u_1)\lambda_T(\xi_7-\xi_1)\frac{S}{N}\\ \quad+(1-u_3)\beta_c\lambda_c(\xi_5-\xi_2)\frac{E_c}{N}+(\mu_H+\phi_{CT})\xi_6\\ \quad+(1-u_3)\beta_T\lambda_T(\xi_5-\xi_7)\frac{E_T}{N}+(1+u_5)\alpha_c(\xi_6-\xi_3)\\ \quad+(1+u_4)\alpha_T(\xi_6-\xi_9)+\omega_{CT}(\xi_6-\xi_1)-c_7,\\ \dot\xi_7=(1-u_2)\lambda_c(\xi_2-\xi_1)\frac{S}{N}+(1-u_1)\lambda_T(\xi_7-\xi_1)\frac{S}{N}\\ \quad+(1-u_3)\beta_c\lambda_c(\xi_5-\xi_2)\frac{E_c}{N}\\ \quad+(1-u_3)\beta_T\lambda_T(\xi_5-\xi_7)\frac{E_T}{N}+(1-u_3)\beta_T\lambda_T(\xi_7-\xi_5)\\ \quad+\theta_R(\xi_7-\xi_9)+\theta_U(\xi_7-\xi_8)+\mu_H\xi_7-c_3,\\ \dot\xi_8=(1-u_2)\lambda_c(\xi_2-\xi_1)\frac{S}{N}+(1-u_1)(\Lambda_T-\lambda_T)(\xi_1-\xi_7)\frac{S}{N}\\ \quad+(1-u_3)\beta_c\lambda_c(\xi_5-\xi_2)\frac{E_c}{N}+(\mu_H+\phi_{TU})\xi_8\\ \quad+(1-u_3)\beta_T(\Lambda_T-\lambda_T)(\xi_7-\xi_5)\frac{E_T}{N}+\alpha_{TU}(\xi_8-\xi_{10})\\ \quad+\omega_{TU}(\xi_8-\xi_1)+\gamma_{TU}(\xi_8-\xi_6)-c_5,\\ \dot\xi_9=(1-u_2)\lambda_c(\xi_2-\xi_1)\frac{S}{N}+(1-u_1)\lambda_T(\xi_7-\xi_1)\frac{S}{N}\\ \quad+(1-u_3)\beta_c\lambda_c(\xi_5-\xi_2)\frac{E_c}{N}+(\mu_H+\phi_{TR})\xi_9\\ \quad+(1-u_3)\beta_T\lambda_T(\xi_5-\xi_7)\frac{E_T}{N}+\alpha_{TR}(\xi_9-\xi_6)\\ \quad+\omega_{TR}(\xi_9-\xi_1)+(1+u_4)\alpha_T(\xi_9-\xi_{10})-c_8,\\ \dot\xi_{10}=(1-u_2)\lambda_c(\xi_2-\xi_1)\frac{S}{N}+(1-u_1)\lambda_T(\xi_7-\xi_1)\frac{S}{N}\\ \quad+(1-u_3)\beta_c\lambda_c(\xi_5-\xi_2)\frac{E_c}{N}\\ \quad+(1-u_3)\beta_T\lambda_T(\xi_5-\xi_7)\frac{E_T}{N}+\mu_H\xi_{10},\end{cases} \tag{60}$$

with the final conditions $\xi_i(T),\ i = 1, \ldots, 10$.

The necessary and sufficient optimality conditions are

$$\frac{\partial \mathbb{H}}{\partial u_1^*} = 0, \quad \frac{\partial \mathbb{H}}{\partial u_2^*} = 0, \quad \frac{\partial \mathbb{H}}{\partial u_3^*} = 0, \quad \frac{\partial \mathbb{H}}{\partial u_4^*} = 0 \quad \text{and} \quad \frac{\partial \mathbb{H}}{\partial u_5^*} = 0, \tag{61}$$

which in turns give the optimal controls

$$\begin{aligned}
u_1^* &= max\left\{0, min\left(1, \frac{(\xi_7 - \xi_1)\lambda_{_T} S}{w_1}\right)\right\},\\
u_2^* &= max\left\{0, min\left(1, \frac{(\xi_2 - \xi_1)\lambda_{_C} S}{w_2}\right)\right\},\\
u_3^* &= max\left\{0, min\left(1, \frac{(\xi_5 - \xi_2)\beta_{_C}\lambda_{_C} E_{_C} + (\xi_5 - \xi_7)\beta_{_T}\lambda_{_T} E_{_T}}{w_3}\right)\right\},\\
u_4^* &= max\left\{0, min\left(1, \frac{(\xi_6 - \xi_9)\alpha_{_T} I_{_{CT}} + (\xi_9 - \xi_{10})\alpha_{_T} I_{_{TR}}}{w_3}\right)\right\},\\
u_5^* &= max\left\{0, min\left(1, \frac{(\xi_6 - \xi_3)\alpha_{_C} I_{_{CT}} + (\xi_3 - \xi_{10})\alpha_{_C} I_{_{CR}}}{w_3}\right)\right\}.
\end{aligned} \tag{62}$$

5. Numerical simulations

To support the analytical results, the optimal control model system 4 is simulated using the model parameter values in Table 1. The positive weight constant $w_1 = w_2 = w_3 = w_4 = w_5 = 2$.

To investigate the impact of various control strategies to mitigate the spread of both diseases, the following five scenarios are considered.

1. Strategy A: COVID-19 prevention and treatment ($u_2 \neq 0, u_5 \neq 0$);
2. Strategy B: COVID-19 prevention, treatment and control of co-infection ($u_2 \neq 0, u_3 \neq 0, u_5 \neq 0$);
3. Strategy C: Tuberculosis prevention and treatment ($u_1 \neq 0, u_4 \neq 0$));
4. Strategy D: Tuberculosis prevention, treatment and control of co-infection ($u_1 \neq 0, u_3 \neq 0, u_4 \neq 0$); and
5. Strategy E: COVID-19 prevention with both TB and COVID-19 treatment ($u_2 \neq 0, u_4 \neq 0, u_5 \neq 0$).

For all the five strategies, the reproduction number calculated using model parameter values in Table 1 is $R_{0_{CT}} = \max(R_{0_C}, R_{0_T}) = 5.8038 > 1$.

5.1. Strategy A: COVID-19 prevention and treatment ($u_2 \neq 0, u_5 \neq 0$)

Simulations of the optimal control system 4 when the strategy that prevents COVID-19 infection ($u_2 \neq 0$) and the treatment of COVID-19 ($u_5 \neq 0$) are implemented. The results of this strategy are shown in Figs. 4, 5, 6, 7 and 8, respectively. When this intervention strategy is implemented, the number of symptomatic individuals not reported I_{cu} drastically decreases, mainly due to the high disease (COVID-19-induced death rate reported in this class). Strategy A could reduce by 1,820 the number of new cases of reported COVID-19 (Fig. 5), and by 600 the number of new co-infections (Fig. 8). The control profiles depicted in Fig. 9 show that treatment is at optimal from the onset of the implementation and remain so throughout, while COVID-19 prevention drops at around 180 days for few days before picking up again. This drop likely corresponds to the relaxation of the COVID-19 prevention measures at the end of the first wave, while the sharp increase corresponds to the beginning of the second COVID-19 wave. For this strategy, we choose the positive weight constants $c_1 = 1.134, c_2 = 1, c_3 = 1, c_4 = 2, c_5 = 1, c_6 = 2, c_7 = 1, c_8 = 1$. Percentage estimation of the cost components of this Strategy A is as follows: unreported COVID-19 symptomatic 20% of the total cost of this strategy, reported symptomatic COVID-19 individuals 20%, co-infected 10%. This strategy does not reduce the number of people infected with tuberculosis as shown in Figs. 6 and 7.

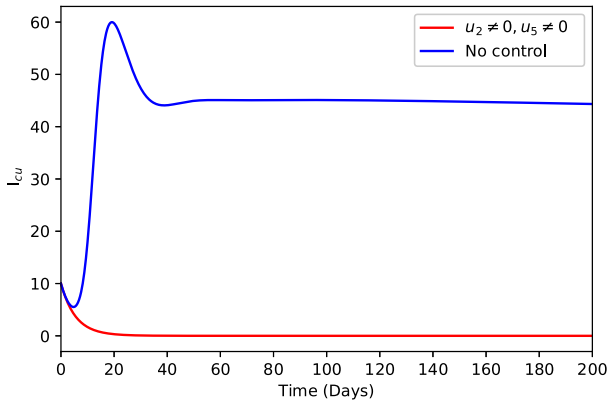

Fig. 4. Individuals I_{cu} with strategy A.

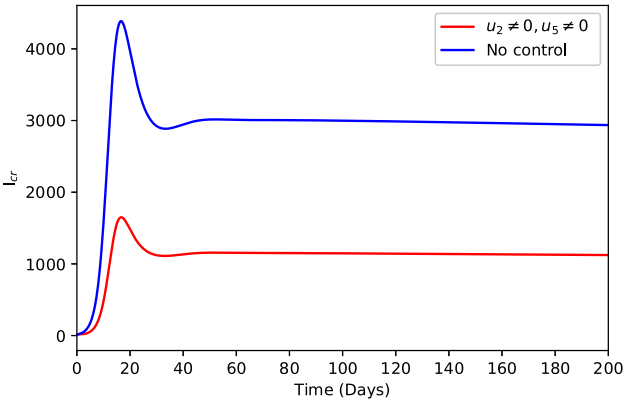

Fig. 5. Individuals I_{cr} with strategy A.

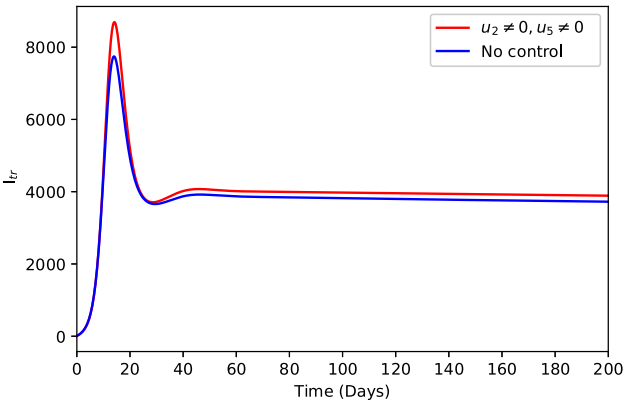

Fig. 6. Individuals I_{tr} with strategy A.

Because the optimal control Figs. 4, 5, 6, 7 and 8 are similar in the remaining strategies, we will only discuss the results without displaying the figures for the sake of avoiding redundancy of graphs.

5.2. Strategy B: COVID-19 prevention, treatment and control of co-infection ($u_2 \neq 0, u_3 \neq 0, u_5 \neq 0$)

Simulations of the optimal control system 4 when the strategy that prevents COVID-19 infection ($u_2 \neq 0$), the treatment of COVID-19 ($u_5 \neq 0$) and control against co-infection ($u_3 \neq 0$) are implemented. When this intervention strategy is implemented, it could reduce by 1,830 the number of new cases of reported COVID-19 I_{tr}, and prevent

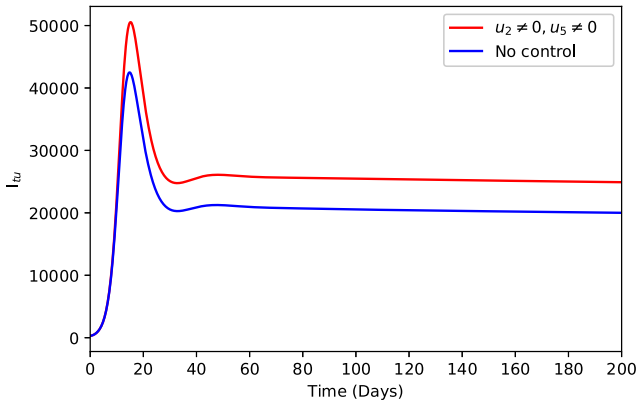

Fig. 7. Individuals I_{tu} with strategy A .

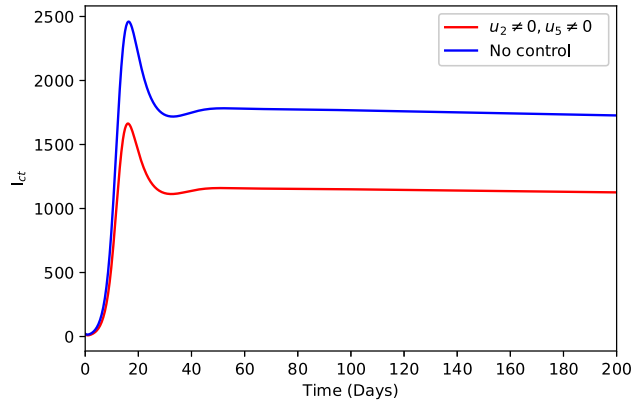

Fig. 8. Co-infected individuals I_{ct} with strategy A.

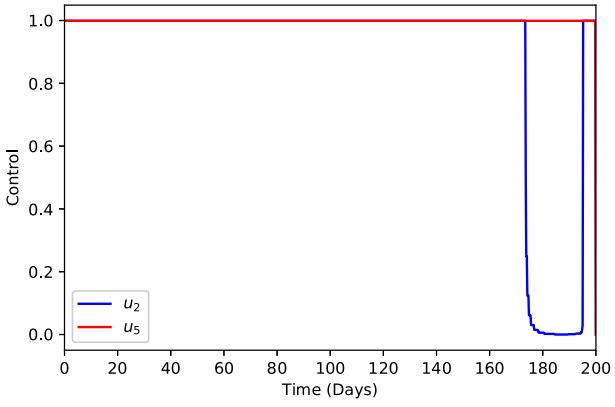

Fig. 9. Control profile for strategy A.

about 615 the number of new co-infections. The number of symptomatic COVID-19 individuals not reported I_{cu} decreases drastically due to the lack of treatment in this class. The control profiles in Fig. 10 show that prevention and treatment are optimal throughout the simulation period, while the control against co-infection is optimal from day 5 and will remain so up to 5 days before the duration of the simulation period. For this strategy, we choose the positive weight constants $c_1 = 1, c_2 = 1, c_3 = 1, c_4 = 1, c_5 = 1, c_6 = 1, c_7 = 1, c_8 = 1$. Percentage estimation of the cost components of Strategy B is as follows: both reported and unreported COVID-19 symptomatic as well as co-infected individuals 12.5% each. As in Strategy A, this strategy also does not reduce the number of people infected with tuberculosis.

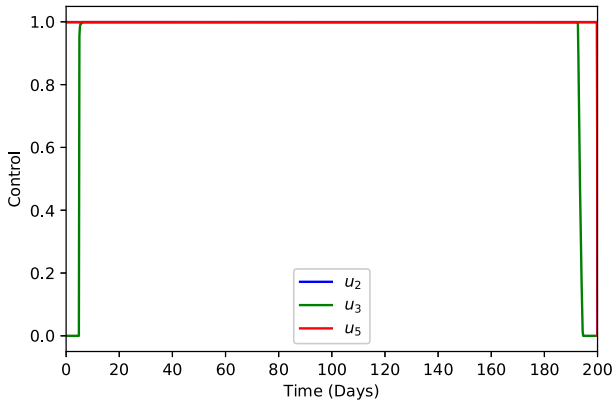

Fig. 10. Control profile for strategy B.

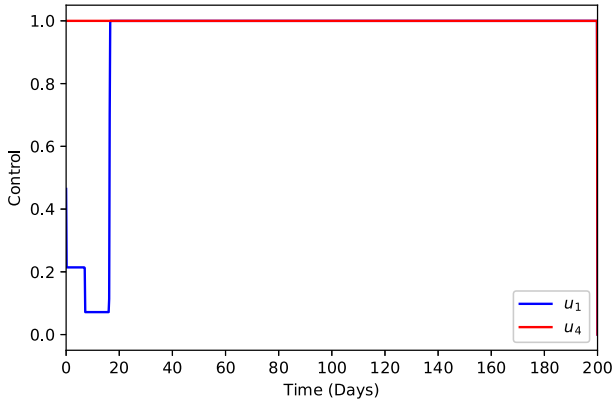

Fig. 11. Control profile for strategy C.

5.3. Strategy C: Tuberculosis prevention and treatment ($u_1 \neq 0, u_4 \neq 0$))

Optimal control simulations for system 4 for Strategy C when tuberculosis prevention and treatment $u_1 \neq 0$ and $u_4 \neq 0$ are implemented. This Strategy C could reduce 2,515 new cases of reported tuberculosis I_{tr}, and 90 new cases of co-infection. The control profiles in Fig. 11 shows that prevention is optimal throughout the simulation period, while treatment is optimal from day 22 through the remainder of the simulation period. For this strategy, we choose the positive weight constants $c_1 = 1, c_2 = 1, c_3 = 1, c_4 = 1, c_5 = 10, c_6 = 1, c_7 = 1, c_8 = 1$. Percentage estimation of the cost components Strategy C is as follows: unreported tuberculosis infected individuals 60% of the total cost of this strategy, reported tuberculosis infected and co-infected individuals 6% each. This strategy does not reduce the number of people infected with COVID-19.

5.4. Strategy D: Tuberculosis prevention, treatment and control of co-infection ($u_1 \neq 0, u_3 \neq 0, u_4 \neq 0$)

Optimal control simulations for system 4 when the strategy for tuberculosis prevention ($u_1 \neq 0$), the treatment of tuberculosis ($u_4 \neq 0$), and control against co-infection ($u_3 \neq 0$) are implemented. This strategy could reduce 2,510 new cases of reported tuberculosis I_{tr}, and by 80 the number of new cases of co-infection. This strategy does not reduce the number of people infected with tuberculosis. The control profiles in Fig. 12 show that control against co-infection which starts approximately from day 10 is optimal throughout the simulation period. The prevention against tuberculosis is optimal from day 105, then decreases between days 154 and 169 (which likely coincides with the peak of COVID-19 first wave), then increases again from day 170.

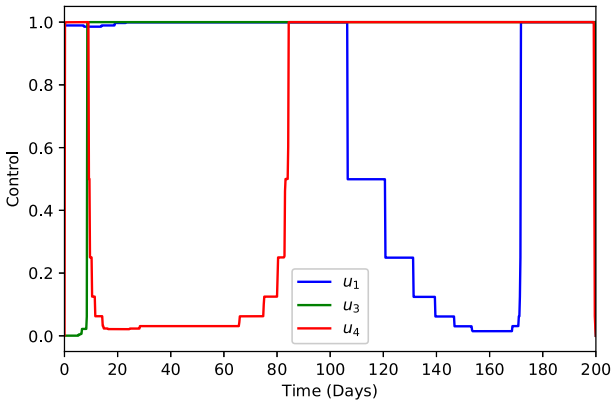

Fig. 12. Control profile for strategy D.

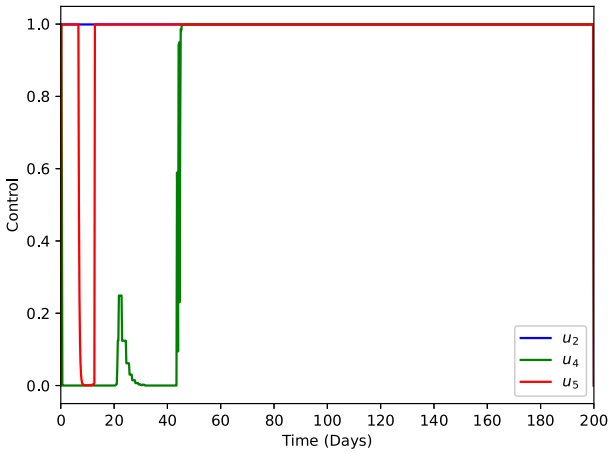

Fig. 13. Control profile for strategy E.

Tuberculosis treatment is optimal for the first 5 days of the simulations, then decreases between days 5 and 65 when we observe an increase that reaches the optimal on day 58. For this Strategy D, we choose the positive weight constants $c_1 = 5, c_2 = 10, c_3 = 5, c_4 = 1, c_5 = 14, c_6 = 1, c_7 = 4, c_8 = 20$. Percentage estimation of the cost components of this strategy is as follows: unreported tuberculosis infected individuals 25% of the total cost of this strategy, reported tuberculosis infected individuals 33.33%, and co-infection 6.66%.

5.5. Strategy E: COVID-19 prevention with both TB and COVID-19 treatment ($u_2 \neq 0, u_4 \neq 0, u_5 \neq 0$)

Optimal control simulations for system 4 for COVID-19 prevention ($u_2 \neq 0$), the treatment of tuberculosis and COVID-19 (respectively $u_4 \neq 0$ and $u_5 \neq 0$) are implemented. This strategy could potentially reduce by 1,520 the number of new cases of reported COVID-19 I_{cr}, 300 new co-infection, and 800 new cases of infected and reported tuberculosis I_{tr}. The control profiles in Fig. 13 show that prevention control of COVID-19 is optimal throughout the simulation period. The COVID-19 treatment is optimal for the first 7 days, then decreases drastically for 5 days and then remains optimal throughout the remainder of the simulation period. Treatment for tuberculosis begins around day 43 and remains at its optimum until the end of the simulation. For this Strategy E, we choose the positive weight constants $c_1 = 7, c_2 = 6, c_3 = 3.5, c_4 = 3.3, c_5 = 1, c_6 = 10, c_7 = 1, c_8 = 1$. Percentage estimation of the cost components of this strategy is as follows: The cost of mitigating the number of unreported COVID-19 infected individuals is 18% of the total cost, reported individuals COVID-19 infected 30%, while co-infection and reported individuals infected with tuberculosis is 3% each. This strategy does not reduce the number of people infected and unreported with tuberculosis.

The outcome of all these strategies are summarized in Table 2. Recall that the model variables in Table 2 are defined as follows:

- $I_{CU}(t)$ unreported individuals infected with COVID-19 only,
- $I_{CR}(t)$ reported individuals infected with COVID-19 only,
- $I_{TU}(t)$ unreported individuals infected with tuberculosis only,
- $I_{TR}(t)$ reported individuals infected with tuberculosis only, and
- $I_{CT}(t)$ co-infected individuals.

Table 2
Summary of the optimal control strategies A - E.

Infections averted	A	B	C	D	E
COVID-19	1,820	1,830	–	–	–
TB	–	–	2,515	2,510	300
Co-infection	600	615	90	80	800
% cost					
$I_{CU}(t)$	20%	12.5%	–	–	18%
$I_{CR}(t)$	20%	12.5%	6%	6.6%	30%
$I_{CT}(t)$	10%	12.5%	–	–	3%
$I_{TU}(t)$	–	–	60%	25%	–
$I_{TR}(t)$	–	–	6%	33.33%	3%

6. Conclusion

We formulated and analyzed a deterministic compartmental model for the transmission dynamics of tuberculosis and COVID-19. Theoretical results show that for both the tuberculosis (31) and COVID-19 only (5) sub-models, the DFE of each sub-model is globally asymptotically stable when the associated basic reproduction numbers R_{0_T} and R_{0_C} are less than unity, unstable otherwise. From the bifurcation analysis (using the central manifold theory), co-existence of both the DFE and the endemic equilibrium is not possible, and consequently, the endemic equilibria of the sub-models are also globally asymptotically stable whenever $R_{0_C} > 1$ and $R_{0_T} > 1$. That is, the bifurcation parameters $a < 0$ and $b > 0$, and the DFE of the two sub-models exchanges their stability with the endemic equilibrium at the threshold $R_{0_C} = 1$ (for the COVID-19 only sub-model (5)) and $R_{0_T} = 1$ (for the tuberculosis only sub-model (31)).

The basic model is then extended to included five control measures. The appropriate conditions for the existence of optimal control and the optimality system for the full model are established using Pontryagin's maximum principle. To support the analytical results, numerical simulations of the model with optimal control are carried out using model parameters from the literature (Table 1).

Five strategies which are a combination of these control measures are investigated. Strategies A and B focus on COVID-19 mitigation, and from Table 2, Strategy B will prevent more COVID-19 and co-infections than Strategy A at a lowest total cost percentage (respectively 2,445; 38% vs 2,420; 50%). Similarly, Strategies C and D focus on TB mitigation. Strategy C will prevent 15 more infections than Strategy D, but at the expense of 7% higher percentage of the total cost of the intervention (2,605; 72% vs 2.590; 65%). Strategy E focuses on both COVID-19 and tuberculosis, and will prevent the least number of infections, 1,110 at 54% of the total cost. Because Strategies C and D focus on tuberculosis mitigation, the results suggest that during the course of the COVID-19 pandemic, Strategy B is a better option compared to Strategies A and E, while Strategies C, D and E will also come at a higher cost. As the COVID-19 pandemic is still ongoing, the best strategy of interest to health policy and decision-makers to mitigate its spread is Strategy B which focuses on COVID-19 prevention, treatment and control of co-infection. This strategy yields a better

outcome in terms of the number of COVID-19 cases prevented at a lower percentage of the total cost.

The proposed model can be extended in several ways by (1) incorporating vaccination against COVID-19 and tuberculosis (2) inflow of infective immigrants (3) exogenous TB re-infection and COVID-19 re-infection after recovery (as several variants have recently emerged), (4) Generally, representations of real-life situations will inherit the loss of information, and sensitivity analysis is warranted. Also, investigating the impact of reducing the transmission rate and speeding up the time to detect infected individual [40].

Declaration of competing interest

The authors declare that they have no known competing financial interests or personal relationships that could have appeared to influence the work reported in this paper.

References

[1] World Health Organization. Tuberculosis keys facts. 2021, http://www.https://www.who.int/en/news-room/fact-sheets/detail/tuberculosis.

[2] Cole E, Cook C. Characterization of infectious aerosols in health care facilities: An aid to effective engineering controls and preventive strategies. Am J Infect Control 1998;26:453–64.

[3] Mtisi E, Rwezaura H, Tchuenche JM. A mathematical analysis of malaria and tuberculosis co-dynamics. Discrete Contin Dyn Syst Ser B 2009;12(4):827–64.

[4] Zu Na, et al. A novel coronavirus from patients with pneumonia in China, 2019. N Engl J Med 2020;382(8):727–33.

[5] Andersen KG, Rambaut A, Lipkin WI, et al. The proximal origin of SARS-CoV-2. Nat Med 2020;26:450–2.

[6] Wu F, Zhao S, Yu B, et al. A new coronavirus associated with human respiratory disease in China. Nature 2020;579:265–9.

[7] World Health Organization. WHO coronavirus (COVID-19) dashboard. 2021, https://covid19.who.int/.

[8] Vanzetti CP, Salvo CP, Kuschner P, Brusca S, Solveyra F, Vilela A. Tuberculosis and COVID-19 coinfection. Medicina (B Aires) 2020;;80(6):100–3.

[9] Swan DA, Bracis C, Janes H, et al. COVID-19 vaccines that reduce symptoms but do not block infection need higher coverage and faster rollout to achieve population impact. Sci Rep 2021;11:15531.

[10] Khurana AK, Aggarwal D. The (in)significance of TB and COVID-19 co-infection. Eur Respir J 2020;56:2002105.

[11] Motta I, Centis R, D'Ambrosio L, et al. Tuberculosis, COVID-19 and migrants: preliminary analysis of deaths occurring in 69 patients from two cohorts. Pulmonology 2020;26:233–40.

[12] Stochino C, Villa S, Zucchi P, Parravicini P, Gori A, Raviglione MC. Clinical characteristics of COVID-19 and active tuberculosis co-infection in an Italian reference hospital. Eur Respir J 2020;56(1):2001708.

[13] Tadolini M, Codecasa LR, Garcia-Garcia JM, et al. Active tuberculosis, sequele and COVID-19 co-infection: first cohort of 49 cases. Eur Respir J 2020;56:2001398.

[14] Tamuzi JL, Ayele BT, Shumba CS, et al. Implications of COVID-19 in high burden countries for HIV/TB: a systematic review of evidence. BMC Infect Dis 2020;20:744.

[15] Guan WJ, Ni ZY, Hu Y, et al. Clinical characteristics of coronavirus disease 2019 in China. N Engl J Med 2020;382:1708–20.

[16] Petrone L, Petruccioli E, Vanini V, Cuzzi G, Gualano G, Vittozzi P, et al. Coinfection of tuberculosis and COVID-19 limits the ability to in vitro respond to SARS-CoV-2. Int J Infect Dis 2021;113(1):S82–87.

[17] Agusto FB. Optimal isolation control strategies and cost-effectiveness analysis of a two-strain avian influenza model. Biosystems 2013;113(3):155–64.

[18] Buonomo B. Analysis of a malaria model with mosquito host choice and bed-net control. Int J Biomath 2015;8(6):1550077.

[19] Zio S, Tougri I, Lamien B. Propagation du COVID19 au burkina faso, modelisation bayesienne et quantification des incertitudes: premiere approche. 2020, preprint, Ecole Polytechnique de Ouagadougou (EPO) Ouagadougou.

[20] Okuonghae D, Aihie V. Case detection and direct observation therapy strategy (DOTS) in Nigeria: its effect on TB dynamics. J Biol Syst 2008;16(1):1–31.

[21] Liu Z, Magal P, Seydi O, Webb GF. Understanding unreported cases in the COVID-19 epidemic outbreak in wuhan, China, and the importance of major health interventions. MPDI Biol 2020;9(50):1–12.

[22] Omame A, Okuonghae D, Umana RA, Inyama SC. Analysis of a co-infection model fo rHPV-TB. Appl Math Model 2020;77:881–901.

[23] Das DK, Khajanchi S, Kar TK. Transmission dynamics of tuberculosis with mupltiple reinfections. Chaos Solitons Fractals 2020;130:109450.

[24] Noor AU, Maqbool F, Bhatti ZA, Khan AU. Epidemiology of CoViD-19 pandemic: Recovery and mortality ratio around the globe. Pak J Med Sci 2020;36(COVID19-S4):S79–84. http://dx.doi.org/10.12669/pjms.36.COVID19-S4.2660.

[25] World Health Organization. Treatment of tuberculosis: Guidelines for nationl programmes. World Health Organization; 2003.

[26] Lansbury L, Lim B, Baskaran V, Lim WS. Co-infections in people with COVID-19: a systematic review and meta-analysis. J Infect 2020;81(2):266–75.

[27] Agusto FB. Optimal chemoprophylaxis and treatment control strategies of a tuberculosis transmission model. World J Model Simul. 2009;5(3):163–73.

[28] Nicholas JI, Adrian ER. Estimating SARS-CoV-2 infections from deaths, confirmed cases, tests, and random surveys. Proceedings of the National Academy of Sciences (PNAS) 2021;18(31):e2103272118.

[29] Sy AAB, Diagne ML, Mbaye I Seydi O. A mathematical model for the impact of public health education campaign for tuberculosis. Far East Journal of Applied Mathematics 2018;100(2):97–138.

[30] Cui J, Tao X, Zhu H. An SIS infection model incorporating media coverage. Rocky Mountain J Math 2008;38(5):1323–34.

[31] Birkhoff G, Rota GC. Ordinary differential equations. 4th ed.. New York: John Wiley and Sons Inc; 1989.

[32] Hutson V, Schmitt K. Permanence and the dynamics of biological systems. Math Biosci 1992;111:1–71.

[33] Mukandavire Z, Gumel AB, Garira W, Tchuenche JM. Mathematical analysis of a model for HIV-malaria co-infection. Math Biosci Engnr 2009;6(2):333–62.

[34] van den Driessche P, Watmough J. Reproduction numbers and sub-threshold endemic equilibria for compartmental models of disease transmission. Math Biosci 2002;180(1):29–48.

[35] Castillo-Chavez C, Song B. Dynamical models of tuberculosis and their applications. Math Biosci Eng 2004;1(2):361–404.

[36] Tchoumi SY, Diagne ML, Rwezaura H, Tchuenche JM. Malaria and COVID-19 co-dynamics: A mathematical model and optimal control. Appl Math Model 2021;99:294–327.

[37] Diagne ML, Rwezaura H, Tchoumi SY, Tchuenche JM. A mathematical model of COVID-19 with vaccination and treatment. Comput Math Methods Med 2021;2021:1250129. http://dx.doi.org/10.1155/2021/1250129.

[38] Franco N. Covid-19 Belgium: Extended SEIR-QD model with nursing homes and long-term scenarios-based forecasts. Epidemics 2021;37:100490.

[39] Pontryagin L, Boltyanskii V, Gamkrelidze R, Mishchenko E. The mathematical theory of optimal control process, vol. 4. New York, London: John Wiley & Sons; 1962.

[40] Ndii MZ, Hadisoemarto P, Dwi Agustian D, Supriatna AK. An analysis of Covid-19 transmission in Indonesia and Saudi Arabia. Cmm Biomath Sci 2020;3(1):19–27.